DOE/ET/53088/48-R IFSR #48-R

VARIATIONAL METHOD FOR THE THREE-DIMENSIONAL INVERSE EQUILIBRIUM PROBLEM IN TOROIDS

A. Bhattacharjee,
Institute for Fusion Studies

J. C. Wiley
Fusion Research Center
The University of Texas at Austin

and

R. L. Dewar
Princeton Plasma Physics Laboratory

May 1983

VARIATIONAL METHOD FOR THE THREE-DIMENSIONAL INVERSE EQUILIBRIUM PROBLEM IN TOROIDS

A. Bhattacharjee*
Institute for Fusion Studies

J. C. Wiley
Fusion Research Center
The University of Texas at Austin
Austin, Texas 78712 USA

and

R. L. Dewar**
Plasma Physics Laboratory
Princeton University
Princeton, New Jersey 08544 USA

Abstract

A variational method is developed for three-dimensional magnetostatic equilibria in toroids. We represent equilibria in cylindrical inverse variables $R(v,\theta,\zeta)$, $\phi(v,\theta,\zeta)$, and $Z(v,\theta,\zeta)$, where v is a radial flux surface label, θ, a poloidal angle, and ζ, a toroidal angle. We Fourier-expand in θ and ζ and derive, from the variational principle, a set of ordinary differential equations for the amplitudes in v. Truncation of the infinite Fourier series leads to a reduced set of equations which we solve numerically by collocation to obtain two- and three-dimensional toroidal equilibria.

---

* Permanent Address: Plasma Physics Programme, Physical Research Laboratory, Ahmedabad 380009, India

** Permanent Address: Department of Theoretical Physics, Research School of Physical Sciences, The Australian National University, Canberra ACT 2600, Australia

NOTE

This paper is a revised and augmented version of an earlier paper (Institute for Fusion Studies Report #48, December, 1981) by the same authors. In its earlier form, the paper was conditionally accepted by the Physics of Fluids in July, 1982. The present paper is being re-submitted.

I. INTRODUCTION

The computation of magnetostatic equilibria in toroids is crucial to the study of plasma stability and transport in toroidal devices. In axisymmetric devices like the tokamak, these equilibria are described by the Grad-Shafranov equation

$$\vec{\nabla} \cdot \left(\frac{\vec{\nabla}\Psi}{R^2} \right) + p'(\Psi) + \frac{FF'(\Psi)}{R^2} = 0 , \tag{1}$$

which is commonly solved in cylindrical coordinates (R,ϕ,Z), with ϕ as the ignorable coordinate. It is suggested by the work of Greene, Johnson, and Weimer[1] on tokamak equilibria, however, that a very useful set of coordinates is the magnetic flux surface coordinates (v,θ,ζ), where v is a radial flux surface label, and θ and ζ are, respectively, the poloidal and toroidal angles parameterizing a flux surface. Indeed, since the magnetic surface coordinates are a natural basis for parameterizing a torus, they define the most natural coordinate system in which an equation, such as Eq. (1), may be studied. With this point of view, we will attempt to determine the mapping

$$R = R(v,\theta,\zeta) , \tag{2a}$$

$$\phi = \phi(v,\theta,\zeta) , \tag{2b}$$

$$Z = Z(v,\theta,\zeta) , \tag{2c}$$

for toroidal equilibria, a problem we have called the three-dimensional inverse equilibrium problem in toroids. Figure 1 depicts the two coordinate systems, (R,ϕ,Z) and (v,θ,ζ); both are right-handed.

In a recent paper, Lao, Hirshman, and Wieland[2] have constructed a variational principle for the Grad-Shafranov equation [Eq. (1)]. For the axisymmetric case, which is their concern, they have considered the mapping

$$R = R(v,\theta) \quad , \tag{3a}$$

$$\phi = \zeta \quad , \tag{3b}$$

$$Z = Z(v,\theta) \quad , \tag{3c}$$

which is a particular case of Eqs. (2). They expand R and Z in Fourier series in θ, and derive from their variational principle an infinite set of coupled differential equations for the amplitudes of R and Z in v. By truncating the infinite set, they claim to have obtained approximate but accurate solutions of the Grad-Shafranov equation for a variety of axisymmetric configurations at a fraction of the computer time needed by typical equilibrium solvers.[2,3]

In this paper, we develop a variational method for three-dimensional equlibria in toroids. The method generalizes the approach of Lao, Hirshman, and Wieland to embrace all mappings of the form given by Eqs. (2). Needless to say, the variational principle of Lao, Hirshman, and Wieland is too restrictive to be of use in the general case. The crucial point is to begin with a variational principle for the magnetostatic equations

$$\vec{J} \times \vec{B} = (\vec{\nabla} \times \vec{B}) \times \vec{B} = \vec{\nabla} p \tag{4a}$$

$$\vec{\nabla} \cdot \vec{B} = 0 \quad , \tag{4b}$$

where p is the scalar pressure of a plasma confined by a magnetic field $\vec{B}$, and $\vec{J}$ is the current density. The variational principle we use is described in Sec. II and is originally due to Grad.[4] In Sec. III we convert to inverse variables $R(v,\theta,\zeta)$ $\phi(v,\theta,\zeta)$, and $Z(v,\theta,\zeta)$ and derive the relevant Euler-Lagrange equations. In Sec. IV, we derive the Euler-Lagrange equations for the Fourier amplitudes of the inverse mapping by substituting the Fourier series for R, ϕ, and Z directly into the variational principle. These equations are ordinary differential equations in v and are at the heart of the method proposed here. In Sec. V, we specialize to a particular choice for the toroidal angle. In Sec. VI, we consider the special case of axisymmetric equilibria in order to establish connection with existing literature. In Sec. VII, we discuss possible choices for the radial flux surface label, and the boundary conditions. Section VIII is devoted to a discussion of our numerical scheme. In Sec. IX, we report detailed comparisons with analytic Solov'ev[5] equilibria and perform convergence studies in order to benchmark the present method. Finally, in Sec. X, we present numerical results on three-dimensional stellarator equilibria.

II. VARIATIONAL PRINCIPLE FOR MAGNETOSTATIC EQUILIBRIA

It has been demonstrated by Kruskal and Kulsrud[6] that solutions of the magnetostatic equations [Eqs. (4)] for plasmas bounded spatially have the property that the magnetic field lines lie on nested surfaces which are topologically toroids. Greene and Johnson[7] have shown that

under these conditions the magnetic field $\vec{B}$ may be represented in the "straight field-line" form

$$\vec{B} = \vec{\nabla}\zeta \times \vec{\nabla}\Psi(v) + \vec{\nabla}\Phi(v) \times \vec{\nabla}\theta \quad ,$$

$$\equiv \vec{\nabla}v \times \left(\Phi_v \vec{\nabla}\theta - \Psi_v \vec{\nabla}\zeta\right) \quad , \tag{5}$$

where $\Psi(v)$ and $\Phi(v)$ are, respectively, the poloidal and the toroidal flux functions. (Here, f_x denotes the partial derivative of f with respect to x.) We will now show that the first variation of the functional

$$L = \int_{V_0} d\tau \left(\frac{B^2}{2} - p\right) \quad , \tag{6}$$

defined over the total volume V_0 of a toroidal plasma bounded by a perfectly conducting wall, subject to the constraint,

$$p \equiv p(v) \quad , \tag{7}$$

vanishes if, and only if, the magnetostatic equations are satisfied. Since Eq. (4b) is satisfied identically by the representation of $\vec{B}$ given by Eq. (5), it will suffice to show that a necessary and sufficient condition for extrema of L is given by Eq. (4a).

The first variation of L is given by

$$\delta L = \int_{V_0} d\tau \left[\delta v\left(\Phi_v \vec{J}\cdot\vec{\nabla}\theta - \Psi_v \vec{J}\cdot\vec{\nabla}\zeta - p_v\right) - \delta\theta\Phi_v \vec{J}\cdot\vec{\nabla}v + \delta\zeta\Psi_v \vec{J}\cdot\vec{\nabla}v\right] \quad , \tag{8}$$

using the boundary conditions

$$\hat{n} \times \vec{\nabla}\Psi = \hat{n} \times \vec{\nabla}\Phi = 0 \ , \tag{9a}$$

$$\delta v = 0 \ , \tag{9b}$$

on the conducting wall. Requiring that $\delta L = 0 \ \forall \ \delta v, \delta\theta, \delta\zeta$, we obtain the Euler-Lagrange equations

$$\vec{J}\cdot\left(\Phi_v \vec{\nabla}\theta - \Psi_v \vec{\nabla}\zeta\right) - p_v = 0 \ , \tag{10a}$$

$$\vec{J}\cdot\vec{\nabla}v = 0 \ , \tag{10b}$$

$$\vec{J}\cdot\vec{\nabla}v = 0 \ . \tag{10c}$$

Equations (10b) and (10c) are identical, and represent the equilibrium constraint that the current $\vec{J}$ lies on flux surfaces. That the same equation is obtained by varying θ and ζ independently reflects the degree of freedom allowed in the variational construction of θ and ζ . In order to define these angles uniquely on a given magnetic surface, it is necessary to choose one of them (directly, or indirectly, through some auxiliary geometric constraint such as a specified Jacobian), whereupon the variational principle determines the other angle. Clearly, the optimum choice for the angles should be guided by the requirements of computational accuracy and spatial resolution of the equilibrium at hand, and, of course, the numerical convergence of the method used to compute the equilibrium.

It is seen by combining Eqs. (5), (10a), and (10b) [or (10c)] that

$$\vec{J} \times \vec{B} = \vec{\nabla} p \quad ,$$

which proves that if L is stationary under arbitrary variations subject to the constraints in Eqs. (7) and (9), the Euler-Lagrange equations satisfy the equations of magnetostatics. The argument may be reversed to show that Eq. (4a), along with the constraint given by Eq. (7), implies that $\delta L = 0$ for arbitrary variations.

For computing equilibria by the present method, the variational principle stated above, originally due to Grad, is essentially equilivalent to that of Kruskal and Kulsrud,[6] in which the potential energy functional

$$W = \int_{V_0} d\tau \left(\frac{B^2}{2} + \frac{p}{\gamma - 1} \right) \quad , \tag{11}$$

is extremized under the class $\mathscr{I}$ of ideal Eulerian variations

$$\delta v = -\vec{\xi} \cdot \vec{\nabla} v \quad ,$$

$$\delta p = -\gamma \vec{\nabla} \cdot (p\vec{\xi}) - (\gamma - 1) p_v \delta v \quad ,$$

where $\vec{\xi}(r,t)$ is the virtual displacement, which obeys the boundary condition

$$\hat{n} \cdot \vec{\xi} = 0 \quad ,$$

on the conducting wall confining the plasma. Since γ, the specific

heat of the plasma, does not appear explicitly in Eqs. (4), for computations of equilibria it seems sensible to work with a quadratic form which is independent of γ . The variational principle of Grad does precisely that, and has the same endpoint, namely, the magnetostatic equations, as the variational principle of Kruskal and Kulsrud.

III. VARIABLE INVERSION

Since L is a scalar, it is independent of the coordinate system in which it is expressed. We now transform from the cylindrical coordinate system (R,ϕ,Z) , to the magnetic coordinate system (v,θ,ζ) whereupon, $R(v,\theta,\zeta)$, $\phi(v,\theta,\zeta)$ and $Z(v,\theta,\zeta)$ are the new dependent variables in the functional L . The elements of the metric tensor $g_{ij} \equiv \vec{e}_i \cdot \vec{e}_j$, where $\vec{e}_i = \partial \vec{r}/\partial x_i$, for the transformation from (x,y,z) coordinates to (R,ϕ,Z) coordinates are

$$g_{vv} = R_v^2 + R^2\phi_v^2 + Z_v^2 \quad , \tag{12a}$$

$$g_{v\theta} = R_v R_\theta + R^2\phi_v\phi_\theta + Z_v Z_\theta = g_{\theta v} \quad , \tag{12b}$$

$$g_{\zeta v} = R_\zeta R_v + R^2\phi_\zeta\phi_v + Z_\zeta Z_v = g_{v\zeta} \quad , \tag{12c}$$

$$g_{\theta\theta} = R_\theta^2 + R^2\phi_\theta^2 + Z_\theta^2 \quad , \tag{12d}$$

$$g_{\theta\zeta} = R_\theta R_\zeta + R^2\phi_\theta\phi_\zeta + Z_\theta Z_\zeta = g_{\zeta\theta} \quad , \tag{12e}$$

$$g_{\zeta\zeta} = R_\zeta^2 + R^2\phi_\zeta^2 + Z_\zeta^2 \quad . \tag{12f}$$

The infinitesimal volume element $d\tau$ is given by

$$d\tau = dxdydz = RdRd\phi\,dz = \sqrt{\|g\|}\; dvd\theta\,d\zeta \quad , \tag{13}$$

where

$$\sqrt{\|g\|} \equiv \left(\text{Det } g_{ij}\right)^{1/2} = R\Big[R_v\left(\phi_\theta Z_\zeta - Z_\theta \phi_\zeta\right) + R_\theta\left(\phi_\zeta Z_v - Z_\zeta \phi_v\right) + R_\zeta\left(\phi_v Z_\theta - Z_v \phi_\theta\right)\Big] \quad . \tag{14}$$

By straightforward manipulations, we get

$$\begin{aligned} L &\equiv \int_0^a dv \int_0^{2\pi} d\theta \int_0^{2\pi} d\zeta \; \mathscr{L}\left(R, R_v, R_\theta, R_\zeta, \phi_v, \phi_\theta, \phi_\zeta, Z_v, Z_\theta, Z_\zeta\right) \\ &= \int_0^a dv \int_0^{2\pi} d\theta \int_0^{2\pi} d\zeta \sqrt{\|g\|} \left[\frac{\Psi_v^2}{2}\frac{g_{\theta\theta}}{\|g\|} + \frac{\Phi_v^2}{2}\frac{g_{\zeta\zeta}}{\|g\|} + \Psi_v \Phi_v \frac{g_{\theta\zeta}}{\|g\|} - p\right] \end{aligned} \tag{15}$$

where $v = a$ is the radial label for the conducting wall, assumed to be fixed. The first variations δR, $\delta\phi$, δZ in the dependent variables $R(v,\theta,\zeta)$, $\phi(v,\theta,\zeta)$, and $Z(v,\theta,\zeta)$ are subject to the fixed boundary constraint given by Eq. (9b), which implies that

$$\delta v = \frac{\partial v}{\partial R}\delta R + \frac{\partial v}{\partial \phi}\delta\phi + \frac{\partial v}{\partial Z}\delta Z = 0 \tag{16a}$$

at $v = a$. From

$$\begin{pmatrix} \delta v \\ \delta\theta \\ \delta\zeta \end{pmatrix} = \left[\frac{\partial(v,\theta,\zeta)}{\partial(R,\phi,Z)}\right] \begin{pmatrix} \delta R \\ \delta\phi \\ \delta Z \end{pmatrix} ,$$

$$= \left[\frac{\partial(R,\phi,Z)}{\partial(v,\theta,\zeta)}\right]^{-1} \begin{pmatrix} \delta R \\ \delta\phi \\ \delta Z \end{pmatrix} ,$$

we get

$$\frac{\partial v}{\partial R} = \frac{R\left(\phi_\theta Z_\zeta - Z_\theta \phi_\zeta\right)}{\sqrt{\| g \|}} \quad ,$$

$$\frac{\partial v}{\partial \phi} = \frac{R\left(Z_\theta R_\zeta - R_\theta Z_\zeta\right)}{\sqrt{\| g \|}} \quad ,$$

and

$$\frac{\partial v}{\partial Z} = \frac{R\left(R_\theta \phi_\zeta - \phi_\theta R_\zeta\right)}{\sqrt{\| g \|}} \quad ,$$

which may be substituted into Eq. (16a) to obtain the condition

$$\left(\phi_\theta Z_\zeta - Z_\theta \phi_\zeta\right)\delta R + \left(Z_\theta R_\zeta - R_\theta Z_\zeta\right)\delta\phi + \left(R_\theta \phi_\zeta - \phi_\theta R_\zeta\right)\delta Z = 0 \qquad (16b)$$

at $v = a$. We note that it is, in general, unduly restrictive and incorrect to require that the variations δR , $\delta\phi$, δZ themselves vanish at the wall, as has been assumed in Ref. 2.

We consider now the first variation of L .

$$\delta L = \int_0^a dv \int_0^{2\pi} d\theta \int_0^{2\pi} d\zeta \sum_{i=1}^{3} \left(\delta f^i \frac{\partial \mathscr{L}}{\partial f^i} + \delta f_v^i \frac{\partial \mathscr{L}}{\partial f_v^i} + \delta f_\theta^i \frac{\partial \mathscr{L}}{\partial f_\theta^i} + \delta f_\zeta^i \frac{\partial \mathscr{L}}{\partial f_\zeta^i} \right) \quad , \qquad (17)$$

where $f^1 = R$, $f^2 = \phi$, and $f^3 = Z$. Integrating by parts, using the single-valuedness of the integrand and the boundary constraint Eq. (16b), we get

$$\delta L = -\int_0^a dv \int_0^{2\pi} d\theta \int_0^{2\pi} d\zeta \sum_{i=1}^{3} \left[\delta f^i \left(\frac{\partial}{\partial v} \frac{\partial \mathscr{L}}{\partial f_v^i} + \frac{\partial}{\partial \theta} \frac{\partial \mathscr{L}}{\partial f_\theta^i} + \frac{\partial}{\partial \zeta} \frac{\partial \mathscr{L}}{\partial f_\zeta^i} - \frac{\partial \mathscr{L}}{\partial f^i} \right) \right] , \tag{18}$$

and the natural boundary constraint at $v = 0$ also given by Eq. (16b). It will be seen that the natural boundary constraint at $v = 0$ is only a weak constraint, and is satisfied identically by a special choice of the radial flux surface label. A necessary and sufficient condition for extrema of L is then given by the Euler-Lagrange equation

$$Q_i \equiv \frac{\partial}{\partial v} \frac{\partial \mathscr{L}}{\partial f_v^i} + \frac{\partial}{\partial \theta} \frac{\partial \mathscr{L}}{\partial f_\theta^i} + \frac{\partial}{\partial \zeta} \frac{\partial \mathscr{L}}{\partial f_\zeta^i} - \frac{\partial \mathscr{L}}{\partial f^i} = 0 \ ;$$

$$i = 1, 2, 3 \ . \tag{19}$$

Using now the definition of $\mathscr{L}$ given by Eq. (15), we obtain the following equations for variations with respect to R, ϕ, and Z, respectively:

$$Q_1 \equiv$$

$$R\left[\left(Z_\theta\phi_\zeta - \phi_\theta Z_\zeta\right)\frac{\partial}{\partial v} + \left(Z_\zeta\phi_v - \phi_\zeta Z_v\right)\frac{\partial}{\partial\theta} + \left(Z_v\phi_\theta - \phi_v Z_\theta\right)\frac{\partial}{\partial\zeta}\right]$$

$$\times\left(\frac{\Psi_v^2}{2}\frac{g_{\theta\theta}}{\|g\|} + \frac{\Phi_v^2}{2}\frac{g_{\zeta\zeta}}{\|g\|} + \Psi_v\Phi_v\frac{g_{\theta\zeta}}{\|g\|} + p\right) + \Psi_v^2\left(\frac{\partial}{\partial\theta}\frac{R_\theta}{\sqrt{\|g\|}} - \frac{R\phi_\theta^2}{\sqrt{\|g\|}}\right)$$

$$+ \Phi_v^2\left(\frac{\partial}{\partial\zeta}\frac{R_\zeta}{\sqrt{\|g\|}} - \frac{R\phi_\zeta^2}{\sqrt{\|g\|}}\right) + \Psi_v\Phi_v\left(\frac{\partial}{\partial\theta}\frac{R_\zeta}{\sqrt{\|g\|}} + \frac{\partial}{\partial\zeta}\frac{R_\theta}{\sqrt{\|g\|}} - \frac{2R\phi_\theta\phi_\zeta}{\sqrt{\|g\|}}\right) = 0 \quad , \tag{20}$$

$$Q_2 \equiv$$

$$R\left[\left(R_\theta Z_\zeta - Z_\theta R_\zeta\right)\frac{\partial}{\partial v} + \left(R_\zeta Z_v - Z_\zeta R_v\right)\frac{\partial}{\partial\theta} + \left(R_v Z_\theta - Z_v R_\theta\right)\frac{\partial}{\partial\zeta}\right]$$

$$\times\left(\frac{\Psi_v^2}{2}\frac{g_{\theta\theta}}{\|g\|} + \frac{\Phi_v^2}{2}\frac{g_{\zeta\zeta}}{\|g\|} + \Psi_v\Phi_v\frac{g_{\theta\zeta}}{\|g\|} + p\right) + \Psi_v^2\frac{\partial}{\partial\theta}\frac{R^2\phi_\theta}{\sqrt{\|g\|}}$$

$$+ \Phi_v^2\frac{\partial}{\partial\zeta}\frac{R^2\phi_\zeta}{\sqrt{\|g\|}} + \Psi_v\Phi_v\left(\frac{\partial}{\partial\theta}\frac{R^2\phi_\zeta}{\sqrt{\|g\|}} + \frac{\partial}{\partial\zeta}\frac{R^2\phi_\theta}{\sqrt{\|g\|}}\right) = 0 \quad , \tag{21}$$

and

$$Q_3 \equiv$$

$$R\left[\left(\phi_\theta R_\zeta - R_\theta\phi_\zeta\right)\frac{\partial}{\partial v} + \left(\phi_\zeta R_v - R_\zeta\phi_v\right)\frac{\partial}{\partial\theta} + \left(\phi_v R_\theta - R_v\phi_\theta\right)\frac{\partial}{\partial\zeta}\right]$$

$$\times\left(\frac{\Psi_v^2}{2}\frac{g_{\theta\theta}}{\|g\|} + \frac{\Phi_v^2}{2}\frac{g_{\zeta\zeta}}{\|g\|} + \Psi_v\Phi_v\frac{g_{\theta\zeta}}{\|g\|} + p\right) + \Psi_v^2\frac{\partial}{\partial\theta}\frac{Z_\theta}{\sqrt{\|g\|}}$$

$$+ \Phi_v^2 \frac{\partial}{\partial \zeta} \frac{Z_\zeta}{\sqrt{\| g \|}} + \Psi_v \Phi_v \left(\frac{\partial}{\partial \theta} \frac{Z_\zeta}{\sqrt{\| g \|}} + \frac{\partial}{\partial \zeta} \frac{Z_\theta}{\sqrt{\| g \|}} \right) = 0 \quad . \tag{22}$$

It is easy to identify Eqs. (20), (21) and (22) as the covariant components of Eq. (4a) in the coordinate system $(\bar{R}, \phi, \bar{Z})$. This may be done by writing Eq. (4a) in the form

$$\vec{\nabla} \left(p + \frac{B^2}{2} \right) - \vec{B} \cdot \vec{\nabla} \vec{B} = 0 \quad , \tag{23}$$

and taking its dot product with $\vec{\nabla} R$, $R\vec{\nabla}\phi$, and $\vec{\nabla} Z$, respectively. We get

$$\vec{\nabla} R \cdot \vec{\nabla} \left(p + \frac{B^2}{2} \right) - \vec{B} \cdot \vec{\nabla} B_R - \frac{B_\phi^2}{R} = 0 \quad , \tag{24}$$

$$R\vec{\nabla}\phi \cdot \vec{\nabla} \left(p + \frac{B^2}{2} \right) - \vec{B} \cdot \vec{\nabla} \left(R B_\phi \right) = 0 \quad , \tag{25}$$

$$\vec{\nabla} Z \cdot \vec{\nabla} \left(p + \frac{B^2}{2} \right) - \vec{B} \cdot \vec{\nabla} B_Z = 0 \quad , \tag{26}$$

where

$$B_R \equiv \vec{B} \cdot \vec{\nabla} R \tag{27a}$$

$$B_\phi \equiv R\vec{B} \cdot \vec{\nabla} \phi \tag{27b}$$

and

$$B_Z = \vec{B} \cdot \vec{\nabla} Z \quad . \tag{27c}$$

If we now use the (operator) equation

$$\vec{B}\cdot\vec{\nabla} = \frac{1}{\sqrt{\|g\|}}\left(\Psi_v \frac{\partial}{\partial\theta} + \Phi_v \frac{\partial}{\partial\zeta}\right) \tag{28}$$

and the identity

$$\frac{\partial(v,\theta,\zeta)}{\partial(R,\phi,Z)}\frac{\partial(R,\phi,Z)}{\partial(v,\theta,\zeta)} = 1 \quad ,$$

it is straightforward to show that Eqs. (20), (21), and (22) are, respectively, identical to Eqs. (24), (25), and (26), written in inverse variables. Furthermore, by combining Eqs. (24), (25), and (26) we obtain

$$\frac{\Psi_v}{\sqrt{\|g\|}}\left[\frac{\partial}{\partial v}\left(\frac{\Psi_v g_{\theta\theta}}{\sqrt{\|g\|}} + \frac{\Phi_v g_{\theta\zeta}}{\sqrt{\|g\|}}\right) - \frac{\partial}{\partial\theta}\left(\frac{\Psi_v g_{v\theta}}{\sqrt{\|g\|}} + \frac{\Phi_v g_{\zeta v}}{\sqrt{\|g\|}}\right)\right]$$

$$+\frac{\Phi_v}{\sqrt{\|g\|}}\left[\frac{\partial}{\partial v}\left(\frac{\Psi_v g_{\theta\zeta}}{\sqrt{\|g\|}} + \frac{\Phi_v g_{\zeta\zeta}}{\sqrt{\|g\|}}\right) - \frac{\partial}{\partial\zeta}\left(\frac{\Psi_v g_{v\theta}}{\sqrt{\|g\|}} + \frac{\Phi_v g_{\zeta v}}{\sqrt{\|g\|}}\right)\right] + p_v = 0 \quad , \tag{29}$$

which is $\vec{J}\times\vec{B} = p_v\vec{\nabla}v$ in inverse variables.

IV. EULER-LAGRANGE EQUATIONS FOR FOURIER AMPLITUDES OF THE INVERSE MAPPING

Exploiting the periodicity of $R(v,\theta,\zeta)$ and $Z(v,\theta,\zeta)$ in θ and ζ, we expand them in Fourier series.

$$R(v,\theta,\zeta) = \sum\Big[R_{m_1,m_2}(v)\cos(m_1\theta - m_2\zeta) + R_{n_1,n_2}(v)\sin(n_1\theta - n_2\zeta)\Big] \tag{30}$$

$$Z(v,\theta,\zeta) = \sum\Big[Z_{p_1,p_2}(v)\cos(p_1\theta - p_2\zeta) + Z_{q_1,q_2}(v)\sin(q_1\theta - q_2\zeta)\Big] \quad , \tag{31}$$

where, unless stated otherwise, the sums extend from $-\infty$ to $+\infty$ over all integers. The generalized toroidal angle ϕ has a secular component which increases by 2π for each toroidal circuit. Apart from this secular component, the angle ϕ may be described by a single-valued function, periodic in θ and ζ. Therefore, we may write

$$\phi = \zeta + \sum \phi_{r_1,r_2}\cos(r_1\theta - r_2\zeta) + \sum \phi_{s_1,s_2}\sin(s_1\theta - s_2\zeta) \tag{32}$$

The first variation of L, formally given by Eq. (18), becomes

$$\begin{aligned}\delta L = -\sum \int_0^a dv \int_0^{2\pi} d\theta \int_0^{2\pi} d\zeta \Big\{ &\Big[\delta R_{m_1,m_2}(v)\cos(m_2\theta - m_2\zeta) + \delta R_{n_1,n_2}(v)\sin(n_1\theta - n_2\zeta)\Big] Q_1 + \Big[\delta\phi_{r_1,r_2}(v)\cos(r_1\theta - r_2\zeta) \\ &+ \delta\phi_{s_1,s_2}(v)\sin(s_1\theta - s_2\zeta)\Big] Q_2 + \Big[\delta Z_{p_1,p_2}(v)\cos(p_1\theta - p_2\zeta) \\ &+ \delta Z_{q_1,q_2}(v)\sin(q_1\theta - q_2\theta)\Big] Q_3\Big\} \quad .\end{aligned}$$

We may now treat $\delta R_{m_1,m_2}$, $\delta R_{n_1,n_2}$, $\delta\phi_{r_1,r_2}$, $\delta\phi_{s_1,s_2}$, $\delta Z_{p_1,p_2}$, and $\delta Z_{q_1,q_2}$, as independent variations to obtain an Euler-Lagrange equation for each Fourier amplitude. These ordinary differential equations, which constitute an infinite set and determine stationary values of L , are

$$\langle\langle \cos(m_1\theta - m_2\zeta) Q_1 \rangle\rangle = 0 , \quad m_1,m_2 \in (-\infty,+\infty) , \tag{33}$$

$$\langle\langle \sin(n_1\theta - n_2\zeta) Q_1 \rangle\rangle = 0 , \quad n_1,n_2 \in (-\infty,+\infty) , \tag{34}$$

$$\langle\langle \cos(r_1\theta - r_2\zeta) Q_2 \rangle\rangle = 0 , \quad r_1,r_2 \in (-\infty,+\infty) , \tag{35}$$

$$\langle\langle \sin(s_1\theta - s_2\zeta) Q_2 \rangle\rangle = 0 , \quad s_1,s_2 \in (-\infty,+\infty) , \tag{36}$$

$$\langle\langle \cos(p_1\theta - p_2\zeta) Q_3 \rangle\rangle = 0 , \quad p_1,p_2 \in (-\infty,+\infty) , \tag{37}$$

$$\langle\langle \sin(q_1\theta - q_2\zeta) Q_3 \rangle\rangle = 0 , \quad q_1,q_2 \in (-\infty,+\infty) , \tag{38}$$

where $\langle\langle\ \rangle\rangle$ is a double-averaging operator defined by

$$\langle\langle A \rangle\rangle \equiv (2\pi)^{-2} \int_0^{2\pi} d\theta \int_0^{2\pi} d\zeta\, A(v,\theta,\zeta) \quad . \tag{39}$$

Equations (33) through (39) are generalization in three dimensions of the variational moment equations derived by Lao, Hirshman, and Wieland for the Grad-Shafranov equation [Eq. (1)]. For numerical computations, we truncate this infinite set by retaining a finite number of terms in the expansions in Eqs. (30), (31), and (32).

V. CHOICE FOR THE TOROIDAL ANGLE

For many cases of interest, such as axisymmetric equilibria or three-dimensional equilibria obtainable by iterating away from axisymmetric equilibria, a convenient choice for the toroidal angle is

$$\phi = \zeta \quad . \tag{40}$$

We may not then vary ϕ in computing δL, given by Eq. (17). For the two independent variations δR and δZ, the Euler-Lagrange equations are now, respectively,

$$\begin{aligned} Q_1 \equiv & \left(RZ_\theta \frac{\partial}{\partial v} - RZ_v \frac{\partial}{\partial \theta}\right)\left(\frac{\Psi_v^2}{2}\frac{g_{\theta\theta}}{\|g\|} + \frac{\Phi_v^2}{2}\frac{g_{\zeta\zeta}}{\|g\|} + \Psi_v\Phi_v\frac{g_{\theta\zeta}}{\|g\|} + p\right) \\ & + \Psi_v^2 \frac{\partial}{\partial\theta}\frac{R_\theta}{\sqrt{\|g\|}} + \Phi_v^2\left(\frac{\partial}{\partial\zeta}\frac{R_\zeta}{\sqrt{\|g\|}} - \frac{R}{\sqrt{\|g\|}}\right) \\ & + \Psi_v\Phi_v\left(\frac{\partial}{\partial\theta}\frac{R_\zeta}{\sqrt{\|g\|}} + \frac{\partial}{\partial\zeta}\frac{R_\theta}{\sqrt{\|g\|}}\right) = 0 \quad , \end{aligned} \tag{41}$$

and

$$\begin{aligned} Q_3 \equiv & \left(-RR_\theta \frac{\partial}{\partial v} + RR_v \frac{\partial}{\partial \theta}\right)\left(\frac{\Psi_v^2}{2}\frac{g_{\theta\theta}}{\|g\|} + \frac{\Phi_v^2}{2}\frac{g_{\zeta\zeta}}{\|g\|} + \Psi_v\Phi_v\frac{g_{\theta\zeta}}{\|g\|} + p\right) \\ & + \Psi_v^2 \frac{\partial}{\partial\theta}\frac{Z_\theta}{\sqrt{\|g\|}} + \Phi_v^2\frac{\partial}{\partial\zeta}\frac{Z_\zeta}{\sqrt{\|g\|}} + \Psi_v\Phi_v\left(\frac{\partial}{\partial\theta}\frac{Z_\zeta}{\sqrt{\|g\|}} + \frac{\partial}{\partial\zeta}\frac{Z_\theta}{\sqrt{\|g\|}}\right) = 0 \quad , \end{aligned} \tag{42}$$

which may be obtained formally by substituting

$$\phi_v = 0 , \quad \phi_\theta = 0 , \quad \phi_\zeta = 1 , \tag{43}$$

in Eqs. (20) and (22). This substitution reduces the degree of nonlinearity of the Euler-Lagrange equations. The elements of the metric tensor g_{ij} are now given by

$$g_{vv} = R_v^2 + Z_v^2 , \tag{44a}$$

$$g_{v\theta} = R_v R_\theta + Z_v Z_\theta = g_{\theta v} , \tag{44b}$$

$$g_{\zeta v} = R_\zeta R_v + Z_\zeta Z_v = g_{v\zeta} , \tag{44c}$$

$$g_{\theta\theta} = R_\theta^2 + Z_\theta^2 , \tag{44d}$$

$$g_{\theta\zeta} = R_\theta R_\zeta + Z_\theta Z_\zeta = g_{\zeta\theta} , \tag{44e}$$

$$g_{\zeta\zeta} = R_\zeta^2 + R^2 + Z_\zeta^2 , \tag{44f}$$

and

$$\sqrt{\| g \|} = R\left(Z_v R_\theta - R_v Z_\theta \right) . \tag{45}$$

Equations (41) and (42) are, as shown before, Eqs. (24) and (26) in inverse variables. We will now prove that the remaining equation, Eq. (25), can be obtained by linear combination of Eqs. (41) and (42). By straightforward algebraic manipulation, we first cast Eqs. (41) and (42) in the form

$$RZ_\theta \left\{ \frac{\Psi_v}{\sqrt{\|g\|}} \left[\frac{\partial}{\partial v} \left(\frac{g_{\theta\theta}\Psi_v}{\sqrt{\|g\|}} + \frac{g_{\theta\zeta}\Phi_v}{\sqrt{\|g\|}} \right) - \frac{\partial}{\partial\theta} \frac{g_{v\theta}\Psi_v}{\sqrt{\|g\|}} \right] + p_v \right.$$

$$+ \frac{\Phi_v}{\sqrt{\|g\|}} \frac{\partial}{\partial v} \left(\frac{g_{\zeta\zeta}\Phi_v}{\sqrt{\|g\|}} + \frac{g_{\zeta\theta}\Psi_v}{\sqrt{\|g\|}} \right) - \frac{\Phi_v}{2\sqrt{\|g\|}} \frac{\partial}{\partial v} g_{\zeta\zeta}$$

$$\left. - \frac{\Psi_v}{\sqrt{\|g\|}} \frac{\partial}{\partial v} g_{\theta\zeta} \right] \Bigg\} - RZ_v\Phi_v \left(\frac{\Phi_v}{2} \frac{\partial}{\partial\theta} \frac{g_{\zeta\zeta}}{\|g\|} + \Psi_v \frac{\partial}{\partial\theta} \frac{g_{\theta\zeta}}{\|g\|} \right)$$

$$+ \Psi_v\Phi_v \left(\frac{\partial}{\partial\theta} \frac{R_\zeta}{\sqrt{\|g\|}} + \frac{\partial}{\partial\zeta} \frac{R_\theta}{\sqrt{\|g\|}} \right) + \Phi_v^2 \left(\frac{\partial}{\partial\zeta} \frac{R_\zeta}{\sqrt{\|g\|}} - \frac{R}{\sqrt{\|g\|}} \right) = 0 \quad , \tag{46}$$

and

$$- RR_\theta \left\{ \frac{\Psi_v}{\sqrt{\|g\|}} \left[\frac{\partial}{\partial v} \left(\frac{g_{\theta\theta}\Psi_v}{\sqrt{\|g\|}} + \frac{g_{\theta\zeta}\Phi_v}{\sqrt{\|g\|}} \right) - \frac{\partial}{\partial\theta} \frac{g_{v\theta}\Psi_v}{\sqrt{\|g\|}} \right] + p_v \right.$$

$$\left. + \frac{\Phi_v}{\sqrt{\|g\|}} \left[\frac{\partial}{\partial v} \left(\frac{g_{\zeta\zeta}\Phi_v}{\sqrt{\|g\|}} + \frac{g_{\zeta\theta}\Phi_v}{\sqrt{\|g\|}} \right) - \frac{\Phi_v}{2\sqrt{\|g\|}} \frac{\partial}{\partial v} g_{\zeta\zeta} - \frac{\Psi_v}{\sqrt{\|g\|}} \frac{\partial}{\partial v} g_{\theta\zeta} \right] \right\}$$

$$+ RR_v\Phi_v \left(\frac{\Phi_v}{2} \frac{\partial}{\partial\theta} \frac{g_{\zeta\zeta}}{\|g\|} + \Psi_v \frac{\partial}{\partial\theta} \frac{g_{\theta\zeta}}{\|g\|} \right)$$

$$+ \Psi_v\Phi_v \left(\frac{\partial}{\partial\theta} \frac{Z_\zeta}{\sqrt{\|g\|}} + \frac{\partial}{\partial\zeta} \frac{Z_\theta}{\sqrt{\|g\|}} \right) + \Phi_v^2 \frac{\partial}{\partial\zeta} \frac{Z_\zeta}{\sqrt{\|g\|}} = 0 \quad . \tag{47}$$

Multiplying Eq. (46) by R_θ, Eq. (47) by Z_θ, and adding the two equations, we get

$$\Phi_v \left(\frac{\partial}{\partial\theta} \frac{g_{\zeta\zeta}}{\sqrt{\|g\|}} - \frac{\partial}{\partial\zeta} \frac{g_{\zeta\theta}}{\sqrt{\|g\|}} \right) + \Psi_v \left(\frac{\partial}{\partial\theta} \frac{g_{\zeta\theta}}{\sqrt{\|g\|}} - \frac{\partial}{\partial\zeta} \frac{g_{\theta\theta}}{\sqrt{\|g\|}} \right) = 0 \quad . \tag{48}$$

Equation (48) may be identified to be the condition

$$\vec{J}\cdot\vec{\nabla}v = \vec{\nabla}\cdot(B\times\vec{\nabla}v) =$$

$$\Phi_v\vec{\nabla}\cdot\left[|\vec{\nabla}v|^2\vec{\nabla}\theta - \vec{\nabla}v(\vec{\nabla}v\cdot\vec{\nabla}\theta)\right] - \Psi_v\vec{\nabla}\cdot\left[|\vec{\nabla}v|^2\vec{\nabla}\zeta - \vec{\nabla}v(\vec{\nabla}v\cdot\vec{\nabla}\zeta)\right] = 0 , \qquad (49)$$

derived earlier as an Euler-Lagrange equation [Eq. (10b) or (10c)] from the variational principle. To complete the proof, we multiply Eq. (41) by $-R_\zeta$, Eq. (42) by $-Z_\zeta$, and add the two equations to get

$$R\left[\left(R_\theta Z_\zeta - Z_\theta R_\zeta\right)\frac{\partial}{\partial v} + \left(R_\zeta Z_v - Z_\zeta R_v\right)\frac{\partial}{\partial\theta}\right]$$

$$\times\left(\frac{\Psi_v^2}{2}\frac{g_{\theta\theta}}{\|g\|} + \frac{\Phi_v^2}{2}\frac{g_{\zeta\zeta}}{\|g\|} + \Psi_v\Phi_v\frac{g_{\theta\zeta}}{\|g\|} + p_v\right) - \Psi_v^2\left(Z_\zeta\frac{\partial}{\partial\theta}\frac{Z_\theta}{\sqrt{\|g\|}} + R_\zeta\frac{\partial}{\partial\theta}\frac{R_\theta}{\sqrt{\|g\|}}\right)$$

$$- \Phi_v^2\left(Z_\zeta\frac{\partial}{\partial\zeta}\frac{Z_\zeta}{\sqrt{\|g\|}} + R_\zeta\frac{\partial}{\partial\zeta}\frac{R_\zeta}{\sqrt{\|g\|}} - \frac{RR_\zeta}{\sqrt{\|g\|}}\right) - \Psi_v\Phi_v\left(Z_\zeta\frac{\partial}{\partial\theta}\frac{Z_\zeta}{\sqrt{\|g\|}} + Z_\zeta\frac{\partial}{\partial\zeta}\frac{Z_\theta}{\sqrt{\|g\|}}\right.$$

$$\left. + R_\zeta\frac{\partial}{\partial\theta}\frac{R_\zeta}{\sqrt{\|g\|}} + R_\zeta\frac{\partial}{\partial\zeta}\frac{R_\theta}{\sqrt{\|g\|}}\right) = 0 . \qquad (50)$$

We now add and subtract

$$R\left(R_vZ_\theta - R_\theta Z_v\right)\frac{\partial}{\partial\zeta}\left(\frac{\Psi_v^2}{2}\frac{g_{\theta\theta}}{\|g\|} + \frac{\Phi_v^2}{2}\frac{g_{\zeta\zeta}}{\|g\|} + \Psi_v\Phi_v\frac{g_{\zeta\theta}}{\|g\|} + p\right)$$

from Eq. (50), and use Eq. (48) to obtain

$$R\left[\left(R_\theta Z_\zeta - Z_\theta R_\zeta\right)\frac{\partial}{\partial v} + \left(R_\zeta Z_v - Z_\zeta R_v\right)\frac{\partial}{\partial\theta} + \left(R_v Z_\theta - Z_v R_\theta\right)\frac{\partial}{\partial\zeta}\right]$$

$$\times\left(\frac{\Psi_v^2}{2}\frac{g_{\theta\theta}}{\|g\|} + \frac{\Phi_v^2}{2}\frac{g_{\zeta\zeta}}{\|g\|} + \Psi_v\Phi_v\frac{g_{\theta\zeta}}{\|g\|} + p\right)$$

$$+ \Phi_v^2\frac{\partial}{\partial\zeta}\frac{R^2}{\sqrt{\|g\|}} + \Psi_v\Phi_v\frac{\partial}{\partial\theta}\frac{R^2}{\sqrt{\|g\|}} = 0 \quad ,$$

which is precisely Eq. (25) in inverse variables. Though demonstrated here for the special case $\phi = \zeta$, Eq. (48) is the general form in inverse variables for $\vec{J}\cdot\vec{\nabla}v = 0$.

VI. AXISYMMETRIC TOROIDAL EQUILIBRIUM

For axisymmetric equilibria, $\partial/\partial\zeta = 0$. The non-vanishing elements of the metric tensor are

$$g_{vv} = R_v^2 + Z_v^2 \quad , \tag{51a}$$

$$g_{v\theta} = R_v R_\theta + Z_v Z_\theta = g_{\theta v} \quad , \tag{51b}$$

$$g_{\theta\theta} = R_\theta^2 + Z_\theta^2 \quad , \tag{51c}$$

$$g_{\zeta\zeta} = R^2 \quad . \tag{51d}$$

Equations (46) and (47) [or equivalently, Eqs. (41) and (42)] then reduce to

$$\mathcal{G}_R \equiv$$

$$RZ_\theta \left[\frac{\Psi_v}{\sqrt{\|g\|}} \left(\frac{\partial}{\partial v} \frac{g_{\theta\theta}\Psi_v}{\sqrt{\|g\|}} - \frac{\partial}{\partial\theta} \frac{g_{v\theta}\Psi_v}{\sqrt{\|g\|}} \right) + \frac{\Phi_v}{\sqrt{\|g\|}} \frac{\partial}{\partial v} \frac{g_{\zeta\zeta}\Phi_v}{\sqrt{\|g\|}} \right.$$

$$\left. + p_v - \frac{\Phi_v^2}{2\|g\|} \frac{\partial}{\partial v} g_{\zeta\zeta} \right] - \frac{\Phi_v^2}{2} RZ_v \frac{\partial}{\partial\theta} \frac{g_{\zeta\zeta}}{\|g\|} - \frac{\Phi_v^2 R}{\sqrt{\|g\|}} = 0 \quad , \tag{52}$$

and

$$\mathcal{G}_Z \equiv$$

$$RR_\theta \left[\frac{\Psi_v}{\sqrt{\|g\|}} \left(\frac{\partial}{\partial v} \frac{g_{\theta\theta}\Psi_v}{\sqrt{\|g\|}} - \frac{\partial}{\partial\theta} \frac{g_{v\theta}\Psi_v}{\sqrt{\|g\|}} \right) + \frac{\Phi_v}{\sqrt{\|g\|}} \frac{\partial}{\partial v} \frac{g_{\zeta\zeta}\Phi_v}{\sqrt{\|g\|}} \right.$$

$$\left. + p_v - \frac{\Phi_v^2}{2\|g\|} \frac{\partial}{\partial v} g_{\zeta\zeta} \right] - \frac{\Phi_v^2}{2} RR_v \frac{\partial}{\partial\theta} \frac{g_{\zeta\zeta}}{\|g\|} = 0 \quad . \tag{53}$$

Equation (48), which is obtained by linear combination of Eqs. (46) and (47), yields the condition

$$\frac{\partial}{\partial\theta} \frac{g_{\zeta\zeta}}{\sqrt{\|g\|}} = 0 \quad , \tag{54}$$

which is not an independent equation once Eqs. (52) and (53) are given, but may be incorporated in the (axisymmetric) variational form at the outset by defining the toroidal field function

$$F(v) \equiv \frac{g_{\zeta\zeta}}{\sqrt{\|g\|}} \Phi_v \quad . \tag{55}$$

If we do so, the two Euler-Lagrange equations, Eqs. (52) and (53), become each identical to

$$\mathcal{G} \equiv \frac{1}{\sqrt{\|g\|}}\left(\frac{\partial}{\partial v}\frac{g_{\theta\theta}\Psi_v}{\sqrt{\|g\|}} - \frac{\partial}{\partial\theta}\frac{g_{v\theta}\Psi_v}{\sqrt{\|g\|}}\right) + \frac{FF_\Psi}{R^2} + p_\Psi = 0 \quad , \tag{56}$$

which is the Grad-Shafranov equation in inverse variables, derived first by Greene, Johnson, and Weimer and used extensively by Lao, Hirshman, and Wieland. We propose, however, to work with Eqs. (52) and (53) because Eq. (48) is not generally reducible to a form as simple as Eq. (54) for three-dimensional equilibria.

For axisymmetric equilibria with up-down symmetry, we must have

$$R(v,\theta) = R(v,-\theta) \quad , \tag{57}$$

$$Z(v,\theta) = -Z(v,-\theta) \quad , \tag{58}$$

The appropriate Fourier expansions for $R(v,\theta)$ and $Z(v,\theta)$ are obtained from Eqs. (30) and (31) by simply substituting $m_2 = n_2 = p_2 = q_2 = n_1 = p_1 = 0$. We have then

$$R(v,\theta) = \sum_{m=0}^{\infty} R_m(v) \cos m\theta \quad , \tag{59}$$

$$Z(v,\theta) = \sum_{p=1}^{\infty} Z_p(v) \sin p\theta \quad , \tag{60}$$

and the Euler-Lagrange equations for the Fourier amplitudes are

$$\langle \cos m\theta \; \mathcal{G}_R \rangle = 0 \quad , \quad m \in (0,\ldots,\infty) \tag{61a}$$

$$\langle \sin p\theta \, \mathcal{G}_Z \rangle = 0 \quad , \quad p \in (1,\ldots,\infty) \tag{61b}$$

where $\langle\ \rangle$ is now defined to be

$$\langle A \rangle \equiv (2\pi)^{-1} \int_0^{2\pi} d\theta \, A(v,\theta) \quad . \tag{62}$$

It should be emphasized again that once the choice of $\phi = \zeta$ has been made, and a radial flux surface label is chosen, Eqs. (61) determine (for up-down symmetric, axisymmetric, equilibria) the angle θ which makes field lines straight. If, however, one uses the representation

$$\vec{B} = \vec{\nabla}\zeta \times \vec{\nabla}\Psi + F\vec{\nabla}\zeta \quad ,$$

as has been essentially done by Lao, Hirshman, and Wieland, the first variations of R and Z each give Eq. (55), which does not by itself determine θ. If one carries through the procedure of Fourier expansion, one obtains the moment equations

$$\langle RZ_\theta \cos m\theta \, \mathcal{G} \rangle = 0 \quad m \in (0,\infty) \tag{63}$$

$$\langle RR_\theta \sin p\theta \, \mathcal{G} \rangle = 0 \quad p \in (1,\infty) \tag{64}$$

which constitute an under-determined set unless θ is specified. This caveat needs to be borne in mind while studying Ref. 2.

The problem of specifying θ may be taken care of by using the convenient representation[2]

$$R = \sum R_m(v) \cos m\theta \tag{65}$$

$$Z = E(v) \sum Z_m(v) \sin m\theta \quad , \tag{66}$$

which contracts the number of independent Fourier amplitudes by implicitly choosing θ . The corresponding moment equations for R_m and E have been derived in Ref. 2, and constitute a well-determined set.

VII. CHOICE OF THE RADIAL FLUX SURFACE LABEL AND BOUNDARY CONDITIONS

The radial flux surface label v is, as yet, unspecified. Any one of the Fourier amplitudes may be used for labelling flux surfaces. Formally, we may not then vary the chosen amplitude while calculating the first variation of L. Instead, the variation of L with respect to Ψ, with $\Phi(\Psi)$ fixed, provides an independent Euler-Lagrange equation

$$\left\langle\!\left\langle \frac{\partial}{\partial v}\frac{\partial \mathscr{L}}{\partial \Psi_v} - \frac{\partial \mathscr{L}}{\partial \Psi} \right\rangle\!\right\rangle = 0 \ , \tag{67}$$

which gives

$$\left\langle\!\left\langle \Psi_v \frac{\partial}{\partial v}\left(\frac{g_{\theta\theta}\Psi_v}{\sqrt{\|g\|}} + \frac{g_{\theta\zeta}\Phi_v}{\sqrt{\|g\|}}\right) + \sqrt{\|g\|}\ p_v \right.\right.$$

$$\left.\left. + \Phi_v \frac{\partial}{\partial v}\left(\frac{g_{\zeta\zeta}\Phi_v}{\sqrt{\|g\|}} + \frac{g_{\zeta\theta}\Psi_v}{\sqrt{\|g\|}}\right)\right\rangle\!\right\rangle = \langle\langle \sqrt{\|g\|}\ Q \rangle\rangle = 0 \ . \tag{68}$$

We identify at once Eq. (68) as the surface-averaged form of Eq. (29).

In what follows, we will examine equilibria which have the group property that if $\theta \to -\theta$ and $\zeta \to -\zeta$, then $R \to R$ and $Z \to -Z$. For axisymmetric systems, the above group property gives us up-down symmetric equilibria. In the three-dimensional case, this implies that in the Fourier series for R and Z given by Eq. (30) and (31), we drop, respectively, all terms proportional to sine and cosine.

We have found it convenient to choose $R_{10} = -|\alpha|v$, where $|\alpha|$ is a positive scaling factor fixed by the geometry of the outermost surface. Having chosen a radial label, we are required to specify boundary conditions for the system of ordinary differential equations comprising (33) (dropping the equation corresponding to $m_1 = 1$, $m_2 = 0$, which is now implied), (38) and (68).

For the Fourier amplitudes, one set of boundary conditions are obtained by Fourier analyzing the outermost flux surface which is held fixed in shape during the iteration. In order that the magnitude of the Fourier coefficients decrease rapidly as the harmonic numbers increase, it is important to choose a poloidal angle $t(\theta,\zeta)$ for Fourier expansion properly. A good choice may be the angle which subtends equal arc-lengths along the projection of the surface on a poloidal plane. The outermost surface is then parameterized as

$$R(v=a,t,\zeta) = \sum \bar{R}^a_{m_1,m_2} \cos(m_1 t - m_2 \zeta) \tag{69a}$$

and

$$Z(v=a,t,\zeta) = \sum \bar{Z}^a_{q_1,q_2} \sin(q_1 t - q_2 \zeta) \tag{69b}$$

The coefficients $\bar{R}^a_{m_1,m_2}$ and $\bar{Z}^a_{q_1,q_2}$ are held fixed during the iteration. The function $t(\theta,\zeta)$ is itself expanded in a Fourier series

$$t = \theta + \sum t_{\alpha_1,\alpha_2} \sin(\alpha_1\theta - \alpha_2\zeta) \tag{69c}$$

and the variational principle may be used to obtain algebraic moment equations for the coefficients t_{α_1,α_2}. Details are given in the Appendix.

The boundary conditions at v=0 are somewhat subtle, because v=0 specifies the magnetic axis, and is, in fact, part of the solution. By performing power-series expansions near v=0 on the equations for the Fourier amplitudes, it is seen that

$$R'_{m_1,m_2}(0) = 0 \qquad (m_1=0) \tag{70a}$$

$$R_{m_1,m_2}(0) = 0 \qquad (m_1\neq 0) \tag{70b}$$

$$Z'_{q_1,q_2}(0) = 0 \qquad (q_1=0) \tag{70c}$$

$$Z_{q_1,q_2}(0) = 0 \qquad (q_1\neq 0) \tag{70d}$$

where $f' \equiv f_v$. These are weak boundary conditions for the Fourier amplitudes at v=0. For Eq. (68), which may be looked upon as an equation for Ψ once the geometry is "frozen", we transform to a new dependent variable

$$u(v) \equiv \frac{\Psi_v}{v} \tag{71}$$

Equation (68) then assumes the form

$$\left(h_1 + \frac{\Phi v}{v}\frac{h_2}{u}\right) u_v + u\, h_{1v} = -\sqrt{\|g\|}\; p_\Psi - \Phi_v\, F_\Psi - \Phi_v\, h_{2v} - \left(h_2 \Phi v/v\right)_v \tag{72}$$

where

$$h_1 \equiv \left\langle\!\left\langle v \frac{g_{\theta\theta}}{\sqrt{\|g\|}} \right\rangle\!\right\rangle \tag{73a}$$

$$h_2 \equiv \langle\langle v \frac{g_{\theta\zeta}}{\sqrt{\| g \|}} \rangle\rangle \tag{73b}$$

$$F \equiv \Phi_v \langle\langle \frac{g_{\zeta\zeta}}{\sqrt{\| g \|}} \rangle\rangle \tag{74}$$

It may be shown by a series expansion that as $v \to 0$, the term proportional to u_v goes to zero faster than the term proportional to u. In the vicinity of $v=0$, Eq. (72) then gives us a simple algebraic equation for u, which is folded into the iteration process and provides a boundary condition for u.

$$u(0) = \lim_{v \to 0} \frac{-\sqrt{\| g \|}\, p_\Psi - \Phi_v F_\Psi - \Phi_v h_{2v} - \left(h_2 \Phi_v / v \right)_v}{h_{1v}} \tag{75}$$

Once u is obtained, we integrate the first-order equation (71), subject to the boundary condition $\Psi(a) \equiv \Psi^a$, to obtain Ψ.

In order to determine any equilibrium, we have to specify two free functions. We present in this paper numerical results for equilibria functions determined by given functions $p(\Psi)$ and $F(\Psi)$. Alternatively, as is done in the study of flux-conserving equilibria, we may specify $p(\Psi)$ and $q(\Psi)$, where $q(\Psi)$ is the q-profile, related to Φ and Ψ through the relation

$$\Phi_v - q\Psi_v = 0 \ . \tag{76}$$

A more physical approach, which shows promise and has been implemented for axisymmetric systems, is to minimize the energy of the plasma

subject to a given set of global constraints. For further details, the reader is referred to Ref. 8, and references therein.

In order to integrate Eq. (74), we need a boundary condition for the toroidal flux function Φ. A natural choice is

$$\Phi(0) = 0 \ . \tag{77}$$

To summarize, Eqs. (33) (excluding the equation corresponding to $m_1=1$, $m_2=0$), (38), (72) and (74), subject to the boundary conditions (70), (75) and (77) constitute a two-point boundary value system, which we solve numerically.

VIII. NUMERICAL METHOD

To solve the two-point boundary-value system of equations referred to in the last section, we use the method of collocation at Gaussian points due to DeBoor and Swartz.[9] We first note that the independent variable v may be scaled by the length a throughout. We, therefore, redefine a dimensionless $v \equiv v/a$, which parameterizes the radial domain $\epsilon[0,1]$. Let $\{f^i(v)\}$ be a finite set of basis functions with support on [0,1]. We define a vector of dependent variables

$$\vec{Y}(v) \equiv (R_{00}, \Psi, Z_{10}, R_{20}, Z_{20}, \ldots.) \tag{78}$$

We expand each dependent variable in a set of N_s basis functions

$$Y_i(v) = \sum_{j=1}^{N_s} a_{ij} f^j(v) \tag{79}$$

and compute the derivatives of $\vec{Y}$ with respect to v. The boundary conditions allow us to determine a subset of the set of coefficients $\{a_{ij}\}$ trivially. The rest are obtained by solving the system of nonlinear ordinary differential equations for $\vec{Y}$ comprising Eqs. (33), (38), (72) and (74), which we represent here abstractly as

$$\vec{F}(\vec{Y}, \vec{Y}_v, \vec{Y}_{vv}) = 0 \tag{80}$$

In order to solve Eq. (80) for the coefficients $\{a_{ij}\}$, we employ a modified Newton's method, which when applied to Eq. (80), gives

$$\overleftrightarrow{A} \cdot (\vec{Y}^{k+1}_{vv} - \vec{Y}^{k}_{vv}) + \overleftrightarrow{B} \cdot (\vec{Y}^{k+1}_{v} - \vec{Y}^{k}_{vv}) + \overleftrightarrow{C} \cdot (\vec{Y}^{k+1} - \vec{Y}^{k}) = \vec{R} \tag{81a}$$

where

$$\overleftrightarrow{A} \equiv \frac{\partial \vec{F}(\vec{Y}^{k}_{vv}, \vec{Y}^{k}_{v}, \vec{Y}^{k})}{\partial \vec{Y}_{vv}} \tag{81b}$$

$$\overleftrightarrow{B} \equiv \frac{\partial \vec{F}(\vec{Y}^{k}_{vv}, \vec{Y}^{k}_{v}, \vec{Y}^{k})}{\partial \vec{Y}_{v}} \tag{81c}$$

$$\overleftrightarrow{C} \equiv \frac{\partial \vec{F}(\vec{Y}^{k}_{vv}, \vec{Y}^{k}_{v}, \vec{Y}^{k})}{\partial \vec{Y}} \tag{81d}$$

and

$$\vec{R} = -\vec{F}(\vec{Y}^{k}_{vv}, \vec{Y}^{k}_{v}, \vec{Y}^{k}) \tag{81e}$$

The essence of a collocation scheme lies in demanding that the differential equations hold at a set of nodes $v=v_k$, known otherwise as collocation points. For the present code, the collocation points are chosen to be the Gaussian quadrature points. The special choice of the collocation points is stated to lead to convergence rates higher than second order.[10] For our purposes, the set of basis functions $\{f^i(v)\}$ is chosen to be the N_s-dimensional space of Hermite cubic B-splines. The number of collocation points $N_c = N_s-2$. A useful summary of the present and other related schemes may be found in the excellent treatise by Strang and Fix.[10]

At every collocation point $v=v_k$, the matrices $\overleftrightarrow{A}$, $\overleftrightarrow{B}$, $\overleftrightarrow{C}$ and $\overleftrightarrow{R}$ are computed after double averaging over the poloidal and the toroidal angles θ and ζ, as indicated by Eq. (39). The angle averages are performed by using Gaussian quadrature. The code is implemented in single precision arithmetic on a VAX-11/780 computer.

IX. COMPARISON WITH ANALYTIC SOLOVEV EQUILIBRIA

In this section we compare the numerical results with analytic Solovév equilibria[5] which are exact solutions of the Grad-Shafranov Equation (1). It may be shown by direct substitution that Eq. (1) has the solution

$$\Psi(R,Z) = F_0\, \ell_0^2\, Z^2 + \frac{P_o}{8}\left(R^2-\ell_o^2\right)^2 \tag{82}$$

if

$$F^2 = 4F_o \ell_o^2(\Psi^a - \Psi) \tag{83a}$$

and

$$p = p_o(\Psi^a - \Psi) \tag{83b}$$

where F_o, p_o and ℓ_o are constants. We note that $\Psi=0$ at the magnetic axis $R=\ell_o$, $Z=0$. This family of analytic equilibria for axisymmetric systems has also been used by Bauer, Betancourt and Garabedian[11] in validating their three-dimensional toroidal code.

We consider a test Solovév equilibrium for which $p_o = 0.125$, $F_o = 0.025$ and $\ell_o = 4$, a case also studied in Ref. 11. In order to represent with acceptable accuracy the outermost flux surface, it is found necessary to include no more than three Fourier coefficients each for R (not counting R_{00}) and Z. The Fourier coefficients for higher harmonics decay approximately exponentially as the harmonic numbers increase. For the present test equilibrium, we use

$$R(v=a,t) = R^a_{00} - |\alpha| \cos t + R^a_{20} \cos 2t + R^a_{30} \cos 3t \tag{84}$$

and

$$Z(v=a,t) = Z^a_{10} \sin t + Z^a_{20} \sin 2t + Z^a_{30} \sin 3t \tag{85}$$

where $R^a_{00} = 3.881$, $|\alpha| = 1.036$, $R^a_{20} = -.0172$, $R^a_{30} = 1.8 \times 10^{-4}$, $Z^a_{10} = 1.569$, $Z^a_{20} = -.0807$ and $Z^a_{30} = -3.89 \times 10^{-3}$.[12] This corresponds to the choice $\Psi^a = 1$, which gives

$$F_o \ell_o^2 Z^2 + \frac{p_o}{8}\left(R^2-\ell_o^2\right)^2 = 1 \qquad (86)$$

as the equation describing the outermost flux surface.

In Fig. 2, we compare the analytical and numerically determined flux surface contours. In Fig. 3 we display the radial profiles of the dominant Fourier amplitudes.

The magnetic axis occurs at R = 3.991, Z=0, which should be compared with the analytical coordinates R = 4, Z=0. We note that the property of approximate exponential convergence, characteristic of the outermost surface, is preserved throughout the radial domain. This is not surprising because there exists a Ψ, analytic in R and Z, for the test problem. In Fig. 4, we plot Ψ as a function of v. The number (or dimension) N_s of radial splines for this run is 16, and the number of collocation points, 14. The number of points in each of the poloidal and toroidal directions for the angle integration is 30.

We report here principally on two types of convergence studies on the test problem. The first study is done by increasing the number of Fourier harmonics holding all other parameters fixed, and, including in the set of harmonics, those for which the contribution to the outermost surface is neglected. In Table 1, we compare the error in Ψ (defined to be $\frac{\max\ |\Psi^N-\Psi|}{\Psi^a}$, where Ψ^N and Ψ are respectively the numerical and exact values of Ψ) as we change the number of Fourier amplitudes. As should be expected, the error decreases as we increase the number of amplitudes.

In Fig. 5, we plot the normalized energy $(2\pi)^{-2}W$, where W is defined according to Eq. (11), as a function of the number of iterations, which is 45 for the runs reported here. The two sets of points correspond to runs made with 7 and 9 Fourier amplitudes.

The second convergence study is performed by changing the number of splines (or collocation points), holding all other parameters fixed. Again, as may be expected, the error in Ψ decreases as the number of splines is increased.

X. THREE-DIMENSIONAL EQUILIBRIA

We present two examples of three-dimensional, toroidal, stellarator equilibria; one, with a planar , and the other, with spatial magnetic axis. Both of these equilibria are obtained by perturbing nontrivially the test Solovev equilibrium by introducing large helical amplitudes on the outermost flux surface. For the case with a planar axis, the outer surface is parameterized as

$$R = R^a_{00} - |\alpha| \cos t + R^a_{20} \cos 2t + R^a_{11} \cos(t-\zeta) \tag{87}$$

$$Z = Z^a_{10} \sin t + Z^a_{20} \sin 2t + Z^a_{11} \sin(t-\zeta) \tag{88}$$

where R^a_{00}, R^a_{20}, Z^a_{10} and Z^a_{20} have the same numerical values as in Eqs. (84) and (85), and $R^a_{11} = Z^a_{11} = 0.333$. In Fig. 7 we show the flux surface contours on different poloidal planes along the axis. Fig. 8 shows the radial profiles of the dominant Fourier amplitudes. In Fig. 9, we plot the normalized energy as a function of the number of iterations. It is seen that in all the plots of energy vs. iteration

number, the approach to the final state is evidently not monotonic. Since the variational principle is a truly minimal principle in the sense that the actual solution will always minimize the energy for stable equilibria, it may appear puzzling that a trial function may give a numerical value for the energy less than the solution. The caveat is that the trial functions violate the boundary condition on u(0), which is folded into the iteration scheme, and is not known ahead of time.

We finally present a stellarator equilibrium with a spatial magnetic axis. The outermost surface is specified by the parametric equations

$$R = R^a_{00} - |\alpha| \cos t + R^a_{20} \cos 2t + R^a_{01} \cos\zeta \tag{89}$$

$$Z = Z^a_{10} \sin t + Z^a_{20} \sin 2t + Z^a_{01} \sin\zeta \tag{90}$$

where R^a_{00}, R^a_{20}, Z^a_{10} and Z^a_{11} have the same numerical values as before, and $R^a_{01} = Z^a_{01} = 0.333$. In Fig. 10, we display the flux surface contours, and in Fig. 11, the radial profiles for the dominant Fourier amplitudes.

There are two defects of the numerical results presented here. The first defect is that some of the Fourier amplitudes seem to exhibit a "boundary-layer" effect, most noticeable, for example, in R_{00}, R_{30} and Z_{30} of Fig. 3, or in R_{00} of Fig. 10. The second defect, not unrelated to the first, is that the residuals of the algebraic equations for t_{α_1,α_2} consistently remain an order of magnitude higher than the residuals for the other equations (which are in the range 10^{-4} - 10^{-7}) at the termination of the computer runs. These residuals do not seem reducible by simply increasing the number of iterations, which shows

that we are not able to improve on the accuracy with which the mapping represented by Eq. (69c) is determined. In an accompanying paper[13], we show how both of these defects may be remedied.

X. CONCLUSIONS

In this paper, we have presented a variational method for computing three-dimensional magnetostatic equilibria. We solve for the inverse variables $R(v,\theta,\zeta)$, $\phi(v,\theta,\zeta)$ and $z(v,\theta,\zeta)$ by Fourier expanding in θ and ζ, and deriving from the variational principle a set of ordinary differential equations for the amplitudes in v. The reduction of a three-dimensional problem to essentially a one-dimensional problem accounts to a large extent for the speed and efficiency of the method. We have presented numerical results for two- and three-dimensional equilibria, and reported on convergence studies in order to establish the validity of the present method.

The use of a variational principle to compute three-dimensional toroidal equilibria, employing magnetic flux coordinates, is not new. The idea was pioneered by Bauer, Betancourt and Garabedian[11] at New York University (N.Y.U.), and has been efficiently used by them in the past few years. The present method is different from the N.Y.U. group's in the choice of the variational principle, but more importantly, in the choice of the dependent variables, and the method by which these variables are solved for. The N.Y.U. group discretizes the energy integral by finite differencing in v, θ and ζ and use an accelerated path of steepest descent in order to arrive at a local minimum-energy state. We Fourier-expand the dependent variables in θ and ζ, and solve the resultant one-dimensional Euler-Lagrange equations. The use of additional damping mechanisms in solving our equations may help in approaching the final state faster, and should be worthwhile to explore. Of course, we must bear in mind that the extra degree of computational

complexity involved in doing so would be worth the return only if it improves markedly the computational efficiency of the method.

The present method converges to a local minimum of the energy functional if the equilibrium is stable. In order to test whether an equilibrium is stable, it is important to test its ruggedness by increasing the number of Fourier amplitudes.

The rigorous validity of the method is predicated on the existence of a flux surface quantity v such that $\vec{B} \cdot \vec{\nabla} v = 0$. The existence of a well-defined direction of symmetry is a sufficient condition for the existence of such flux surfaces. In that case, as we have seen for the axisymmetric equilibrium considered here, the Fourier series for the inverse variables converge rapidly, and there is mathematical proof fortifying such convergence. However, even in the absence of a well-defined direction of symmetry, as is the case with toroidal stellarators, the present method obtains numerically Fourier representations of nested flux surfaces with good convergence properties The question whether such three-dimensional solutions describe rigorous equilibria or "asymptotic" equilibria is difficult to answer within the scope of the present work.

APPENDIX

In this Appendix, we derive from the variational principle algebraic equations for the Fourier amplitudes of t

$$t = \theta + \sum t_{\alpha_1,\alpha_2} \sin(\alpha_1\theta - \alpha_2\zeta) \ . \tag{A1}$$

Near v=a, we constrain δR and δZ to variations in t, according to

$$\delta R = R_t \delta t \ , \tag{A2}$$

and

$$\delta Z = Z_t \delta t \tag{A3}$$

Near v=a, we consider the contribution to the first variation of L, which is proportional to

$$\delta L^a = - \int_0^{2\pi} d\theta \int_0^{2\pi} d\zeta \left[Q_1 R_t + Q_3 Z_t \right] \delta t \ . \tag{A4}$$

Substituting the expansion (A1) directly into (A4), and varying each coefficient α_1,α_2 independently, we obtain the Euler-Lagrange equations

$$\langle\langle \ (Q_1 R_t + Q_3 Z_t) \sin(\alpha_1\theta - \alpha_2\zeta) \ \rangle\rangle = 0 \quad , \quad \alpha_1,\alpha_2 \ \varepsilon \ (-\infty,+\infty) \tag{A5}$$

We note that the Euler-Lagrange equation for t, which is

$$Q_1 R_t + Q_3 Z_t = 0 \quad , \tag{A6}$$

or equivalently

$$t_\theta^{-1}(Q_1 R_\theta + Q_3 Z_\theta) = 0 \quad , \tag{A7}$$

may be identified to be precisely

$$\vec{J}\cdot\vec{\nabla}v = 0 \quad ,$$

if we recall the manipulations leading up to Eq. (48). The procedure outlined above is analogous to that used by Schlüter and Schwenn[14]. The moment Eqs. (A5) have been incorporated in the numerical scheme. In order to assure that the mapping (A1) be monotonic, in the code we constrain the step-size for Eqs. (A5) to satisfy the inequality

$$1 - \sum_{\alpha_1} \alpha_1 < 0 \quad .$$

ACKNOWLEDGMENTS

The first author (A.B.) would like to thank Dr. D. C. Barnes, Dr. J. M. Greene, Dr. J. Nührenberg, and Dr. M. N. Rosenbluth for a few useful discussions. He is grateful to Ms. S. Crumley and Ms. K. S. Al - Sweilem for typing this manuscript.

Some of this work was completed at the Aspen Center of Physics, Colorado, where two of the authors (A.B. and R.L.D.) spent a few enjoyable weeks in the summer of 1982. The hospitality of the staff at Aspen Center is gratefully acknowledged.

This work was primarily supported by the United States Department of Energy under contract #DE-AC05-79ET-53-36 at the Institute for Fusion Studies and contract #DE-FG05080ET-53088 at the Fusion Research Center.

REFERENCES

1. J. M. Greene, J. L. Johnson, and K. E. Weimer, Phys. Fluids 14, 671(1971).

2. L. L. Lao, S. P. Hirshman, and R. M. Wieland, Phys. Fluids 24, 1431(1981).

3. J. A. Holmes, Y-K. M. Peng, and S. J. Lynch, J. Comput. Phys. 36, 35(1980).

4. H. Grad, Phys. Fluids 7, 1283(1964).

5. L. S. Solóvev, [Zh. Eksp. Teor. Fiz. 53, 626(1967)][Sov. Phys. JETP 26, 400(1968)].

6. M. D. Kruskal and R. M. Kulsrud, Phys. Fluids 1, 265(1958).

7. J. M. Greene and J. L. Johnson, Phys. Fluids 5, 510(1962).

8. A. Bhattacharjee and J. C. Wiley, Phys. Fluids 26 (2), 520(1983).

9. C. DeBoor and B. Swartz, SIAM J. Numer Anal. 14, 441(1977).

10. G. Strang and G. J. Fix, An Analysis of the Finite Element Method, Prentice-Hall, Inc. (New York, 1977).

11. F. Bauer, O. Betancourt, and P. Garabedian, A Computational Method in Plasma Physics, Springer-Verlag New York, Inc. (New York, 1978).

12. Referee, private communication.

13. A. Bhattacharjee, J. C. Wiley and R. L. Dewar, to be published.

14. A. Schlüter and U. Schwenn, Computer Physics Communications 24, 263(1981).

FIGURE CAPTIONS

Fig. 1 Two coordinate systems; the cylindrical coordinate system (R,ϕ,Z) and the magnetic coordinate system (v,θ,ζ).

Fig. 2 Comparison of exact (indicated by dots) and numerically determined (indicated by solid lines) flux surfaces for the test Solov́ev equilibrium.

Fig. 3 Radial profiles of the dominant Fourier amplitudes for the equilibrium shown in Fig. 2.

Fig. 4 Radial profile of $\Psi(v)$ for the test Solov́ev equilibrium.

Fig. 5 Energy (normalized) versus number of iterations. The black circles, connected by a line, are obtained by solving for the 6 Fourier amplitudes given in Fig. 4. The unconnected open circles are obtained by solving for 8 Fourier amplitudes.

Fig. 6 Flux contours for a three-dimensional stellarator equilibrium with a planar magnetic axis.

Fig. 7 Radial profiles of the dominant Fourier amplitudes for the equilibrium shown in Fig. 6.

Fig. 8 Energy (normalized) versus number of iterations for the equilibrium shown in Fig. 6.

Fig. 9 Flux surface contours for a three-dimensional stellarator equilibrium with a spatial magnetic axis.

Fig. 10 Radial profiles of the dominant Fourier amplitudes for the equilibrium shown in Fig. 9.

Fig. 1

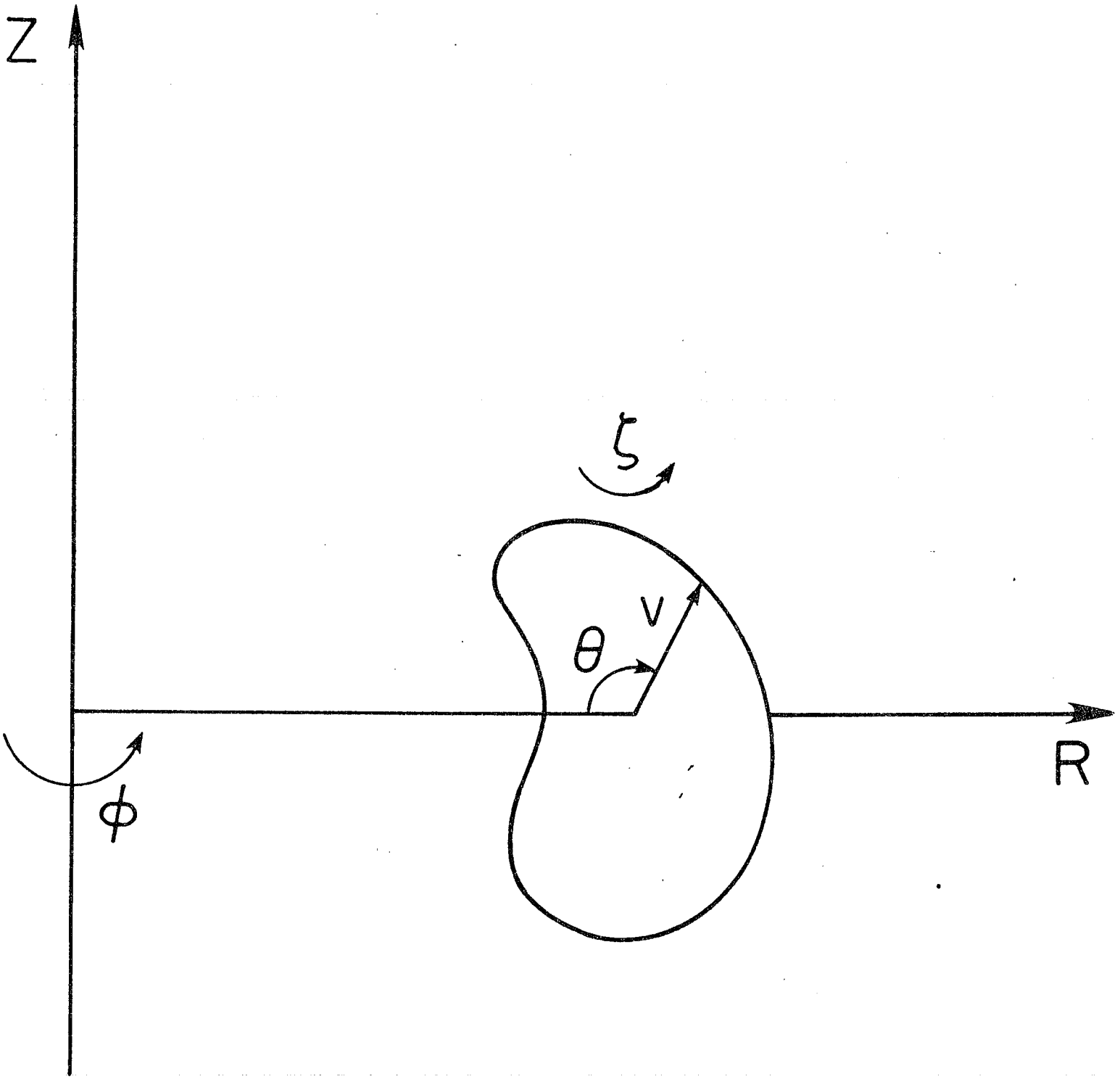

Fig. 2

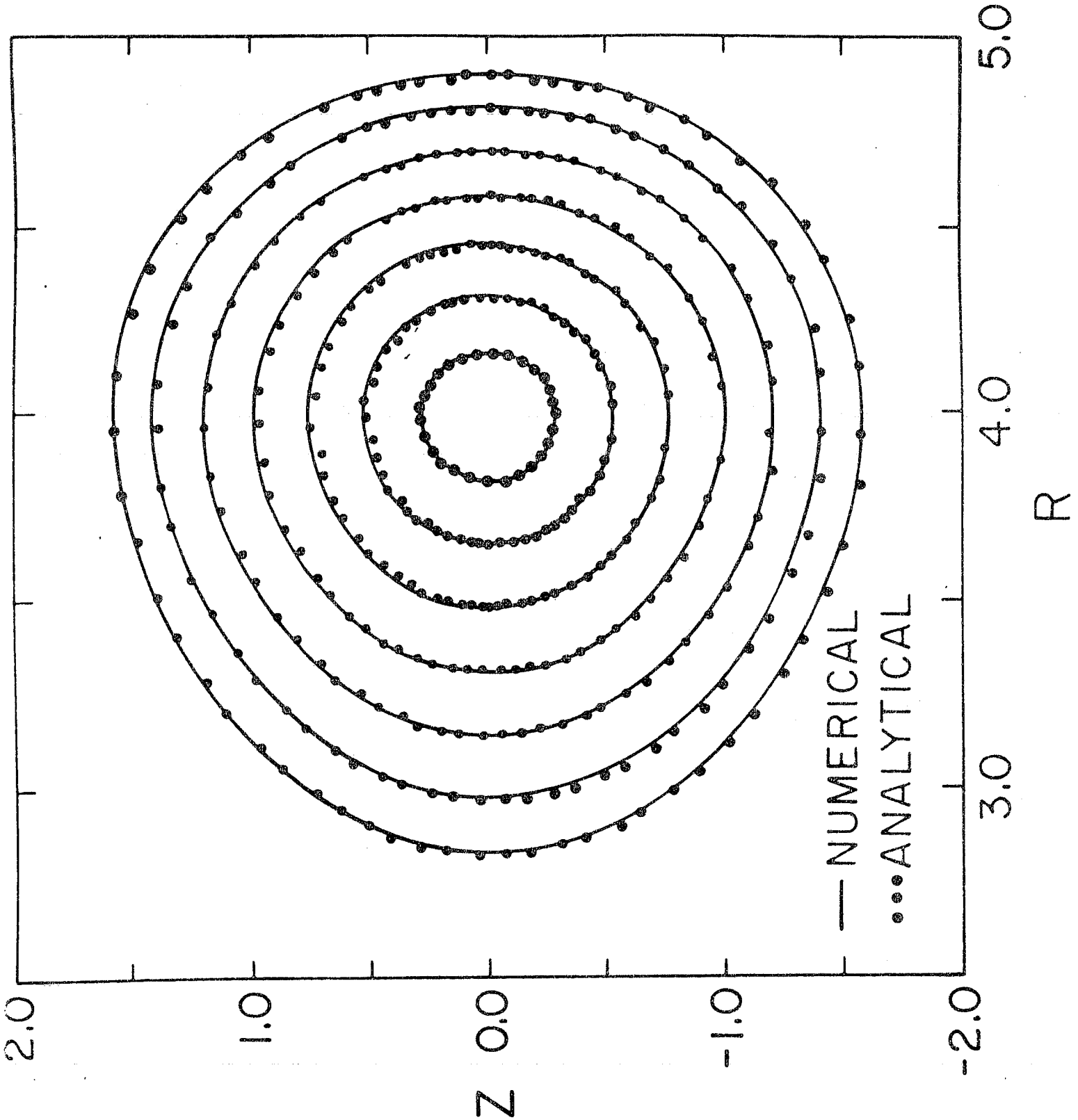

Fig. 3

NORMALIZATION FACTOR FOR

$R_{00} = 3.991$, $R_{20} = 0.092$, $R_{30} = -7.230 \times 10^{-3}$

$Z_{10} = 1.569$, $Z_{20} = -0.196$, $Z_{30} = 2.661 \times 10^{-2}$

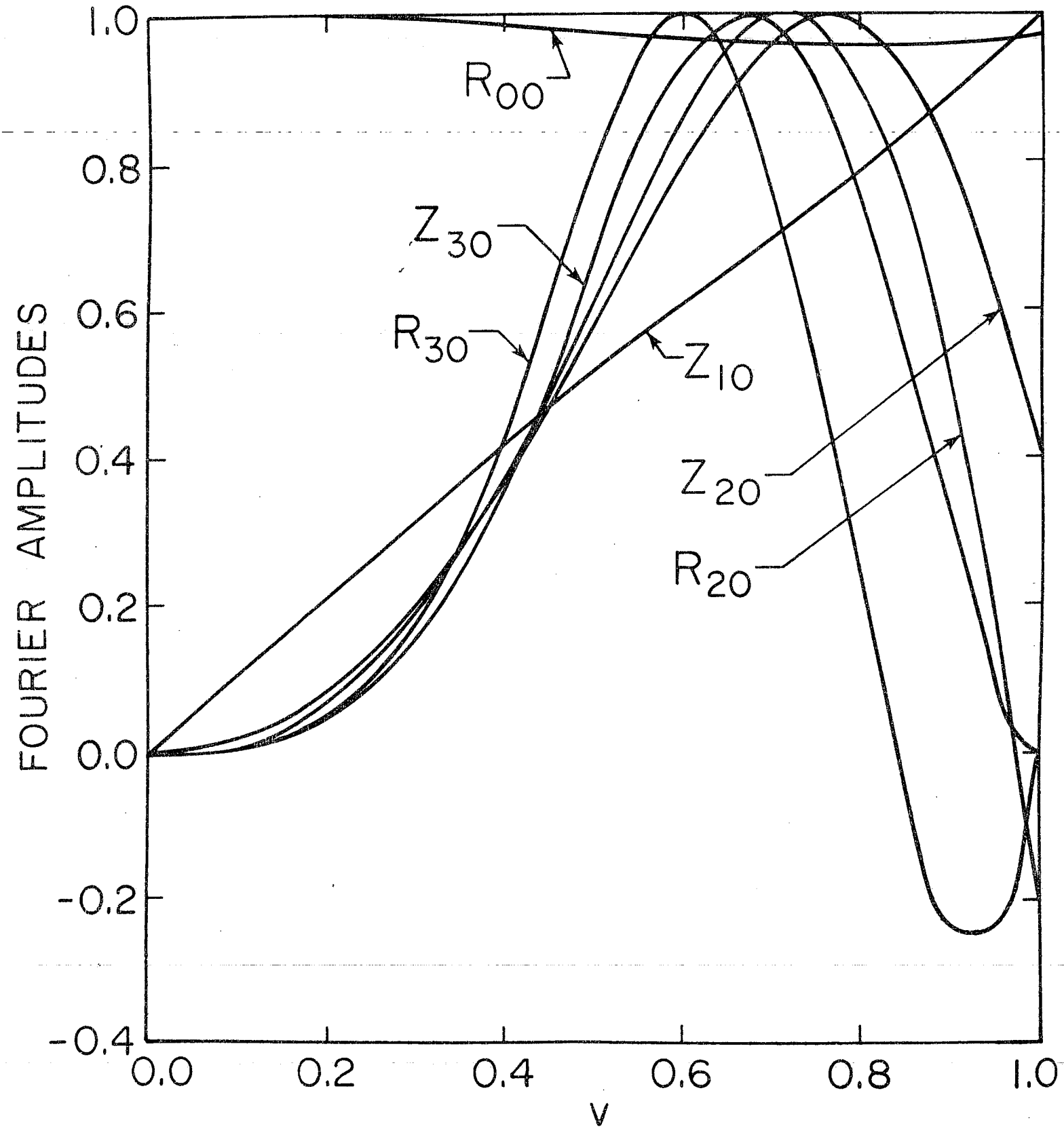

Fig. 4

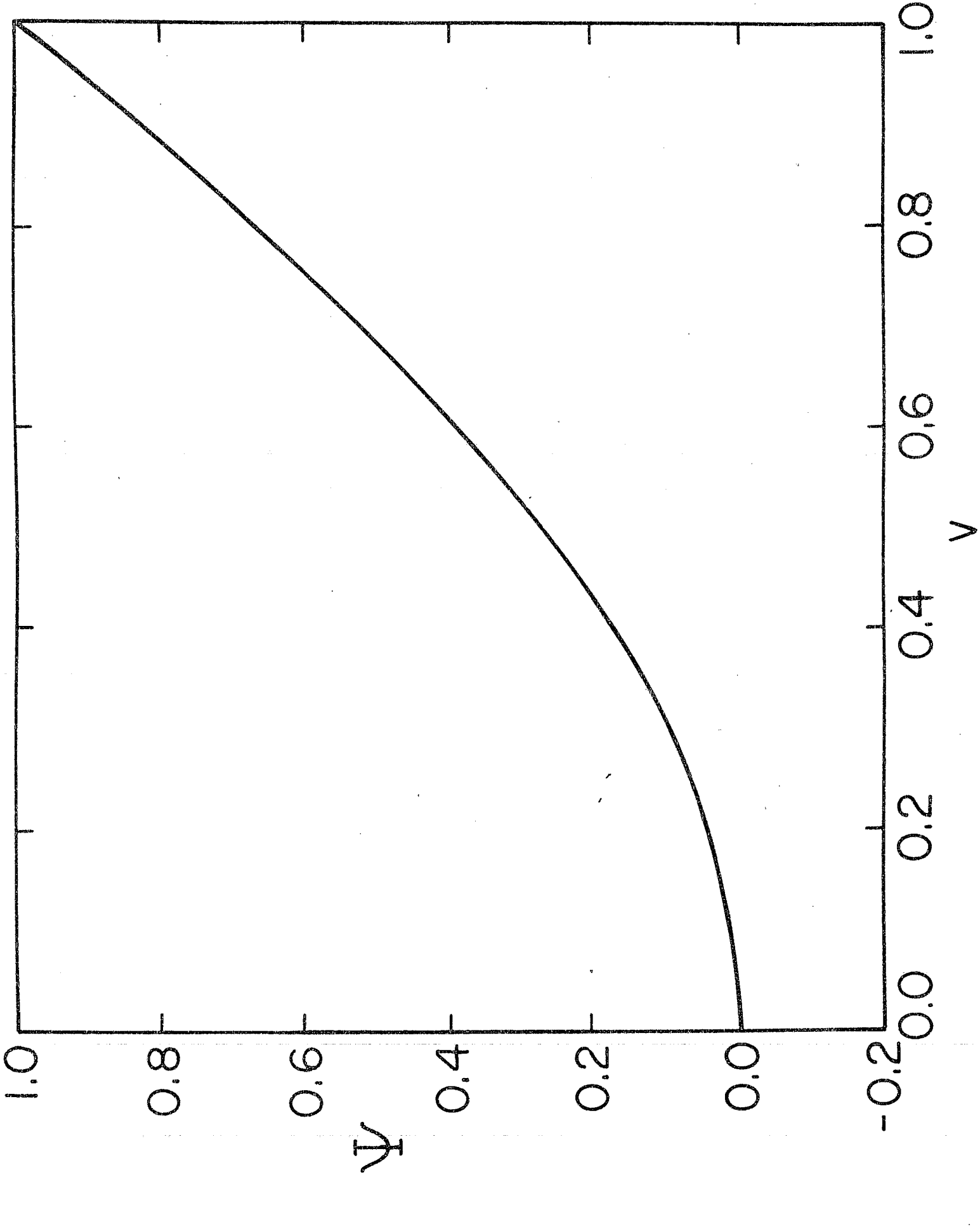

Fig. 5

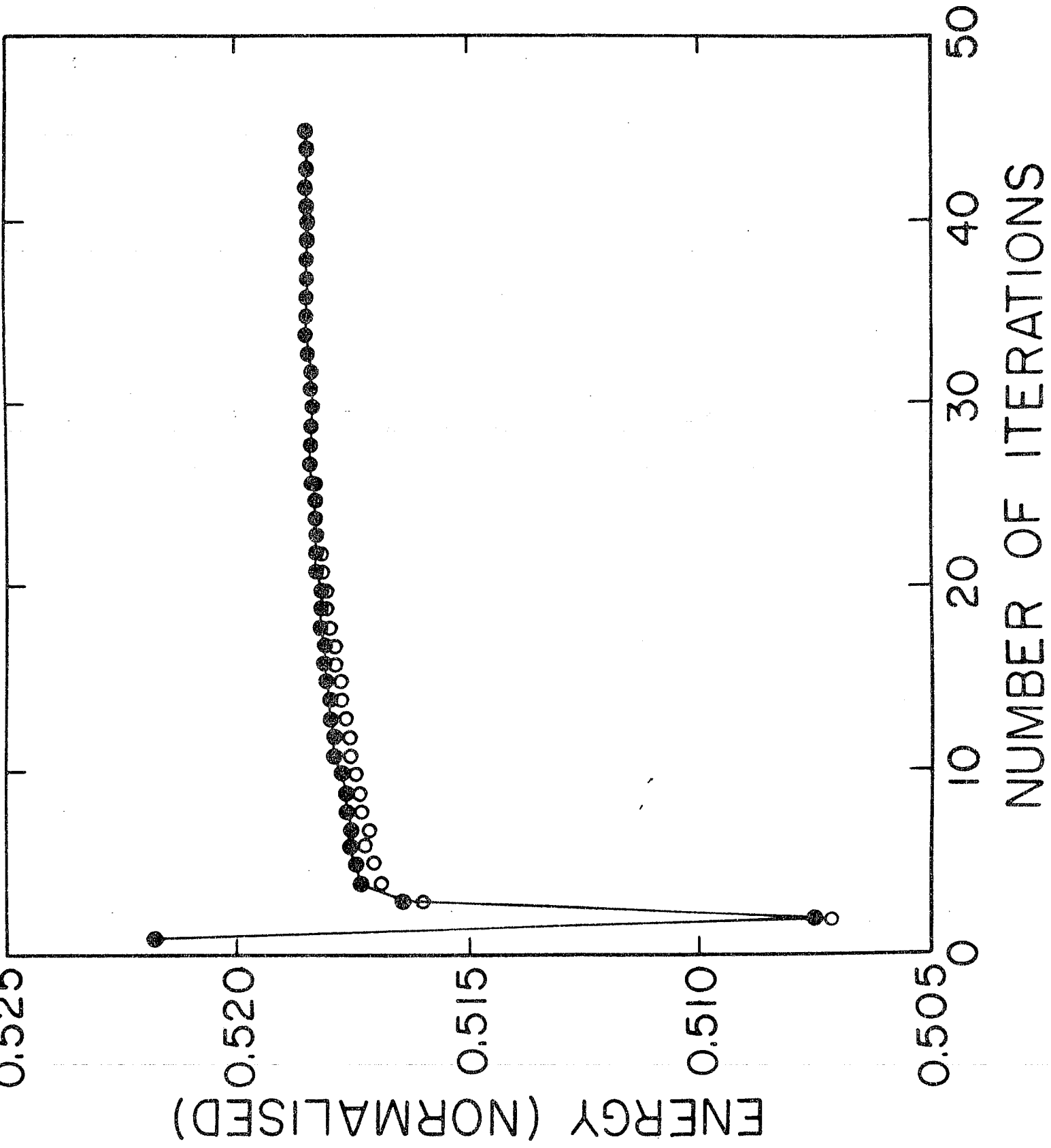
ENERGY (NORMALISED)
0.525
0.520
0.515
0.510
0.505
0
10
20
30
40
50
NUMBER OF ITERATIONS

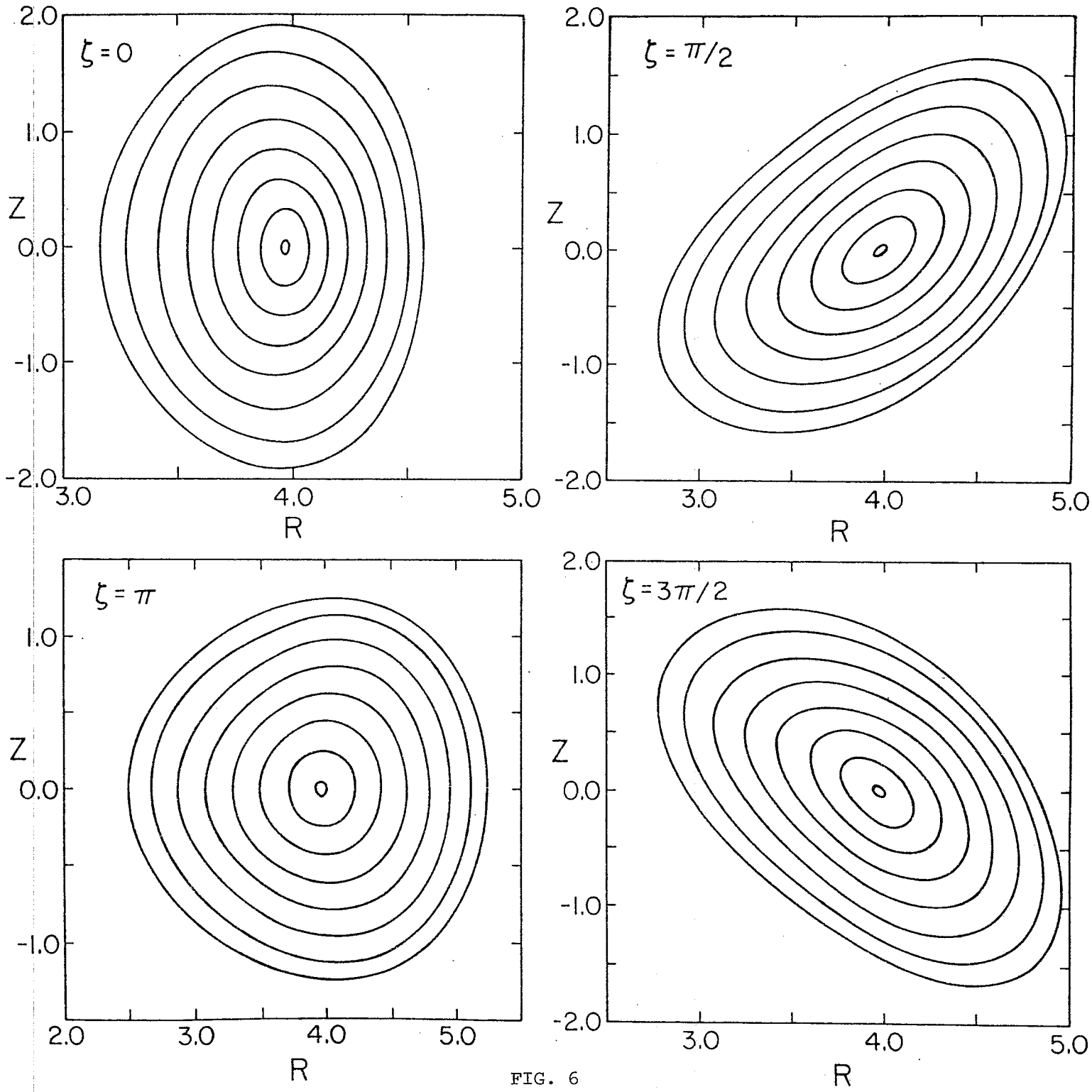

FIG. 6

Fig. 7

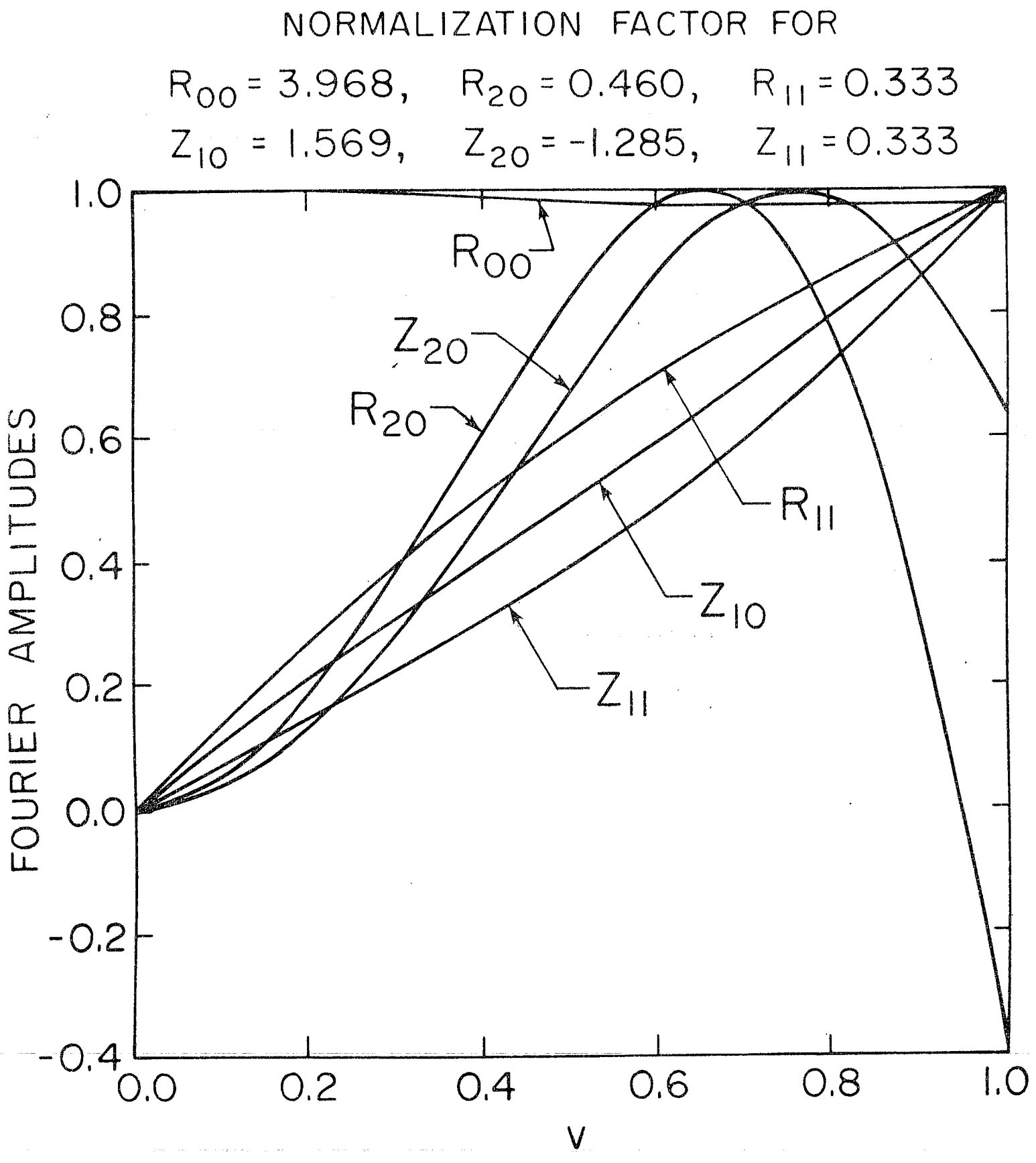
NORMALIZATION FACTOR FOR
$R_{00} = 3.968$, $R_{20} = 0.460$, $R_{11} = 0.333$
$Z_{10} = 1.569$, $Z_{20} = -1.285$, $Z_{11} = 0.333$
FOURIER AMPLITUDES
V
R_{00}
Z_{20}
R_{20}
R_{11}
Z_{10}
Z_{11}
1.0
0.8
0.6
0.4
0.2
0.0
-0.2
-0.4
0.0
0.2
0.4
0.6
0.8
1.0

Fig. 8

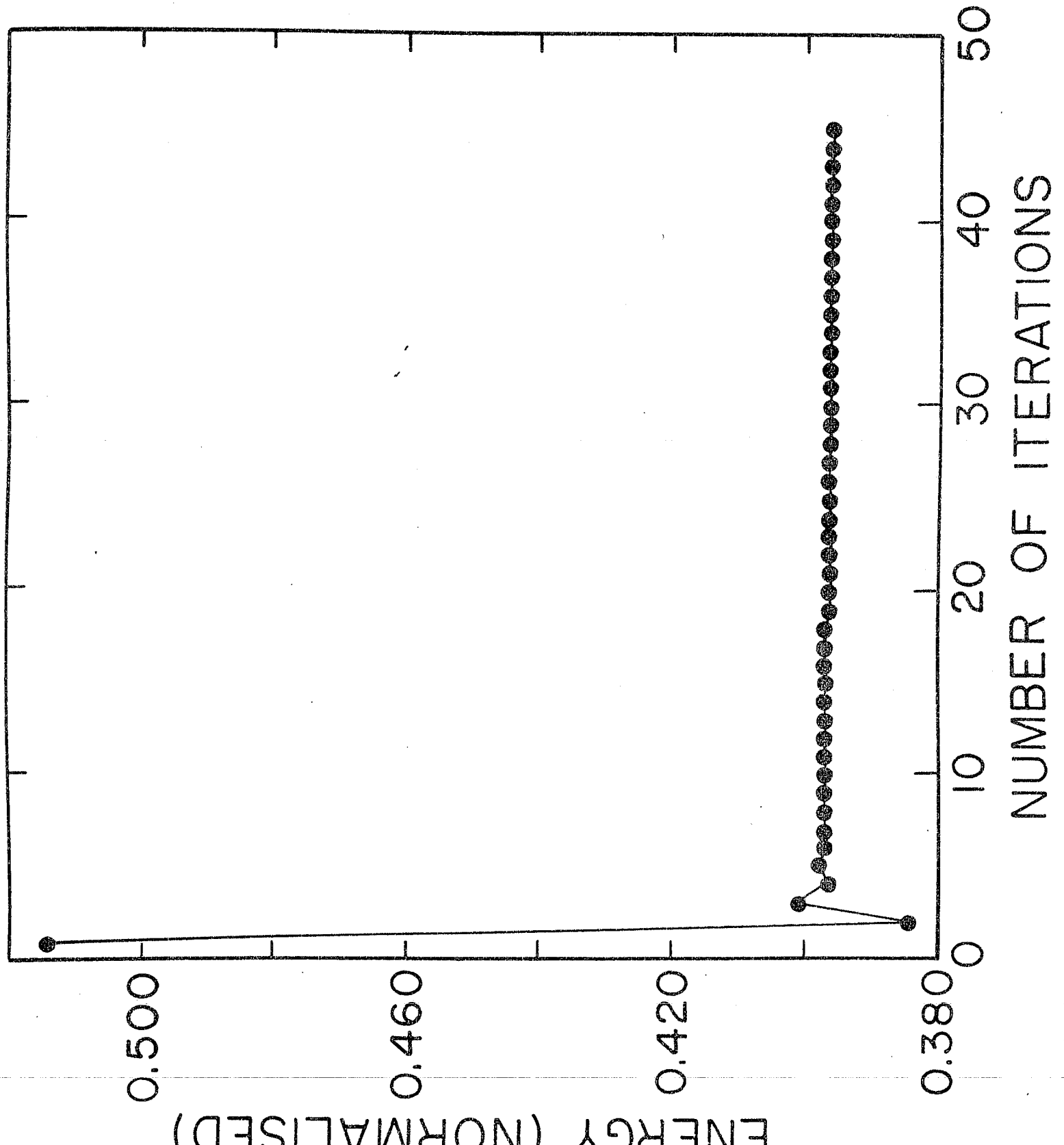
ENERGY (NORMALISED)
0.500
0.460
0.420
0.380
0
10
20
30
40
50
NUMBER OF ITERATIONS

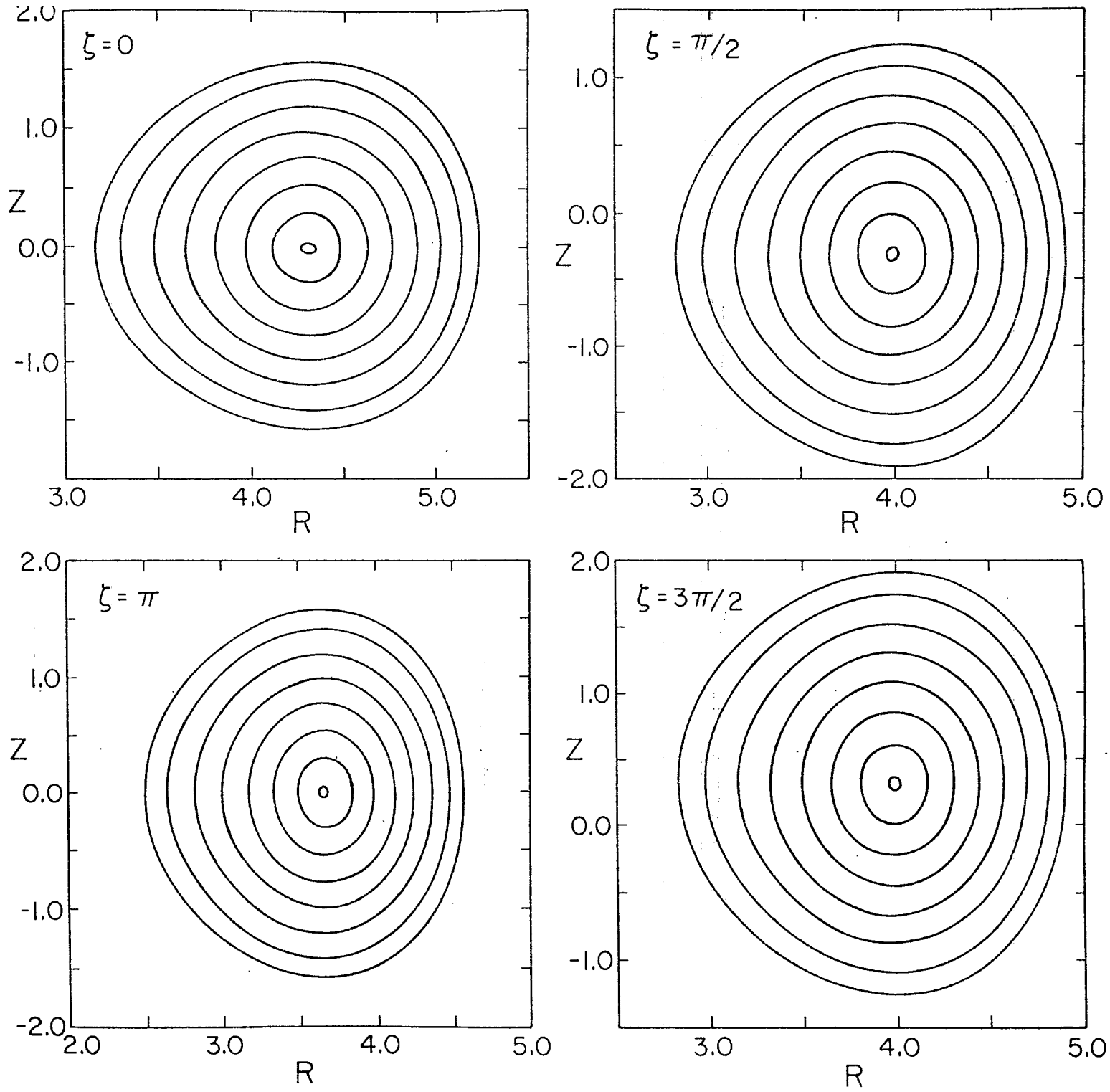

FIG. 9

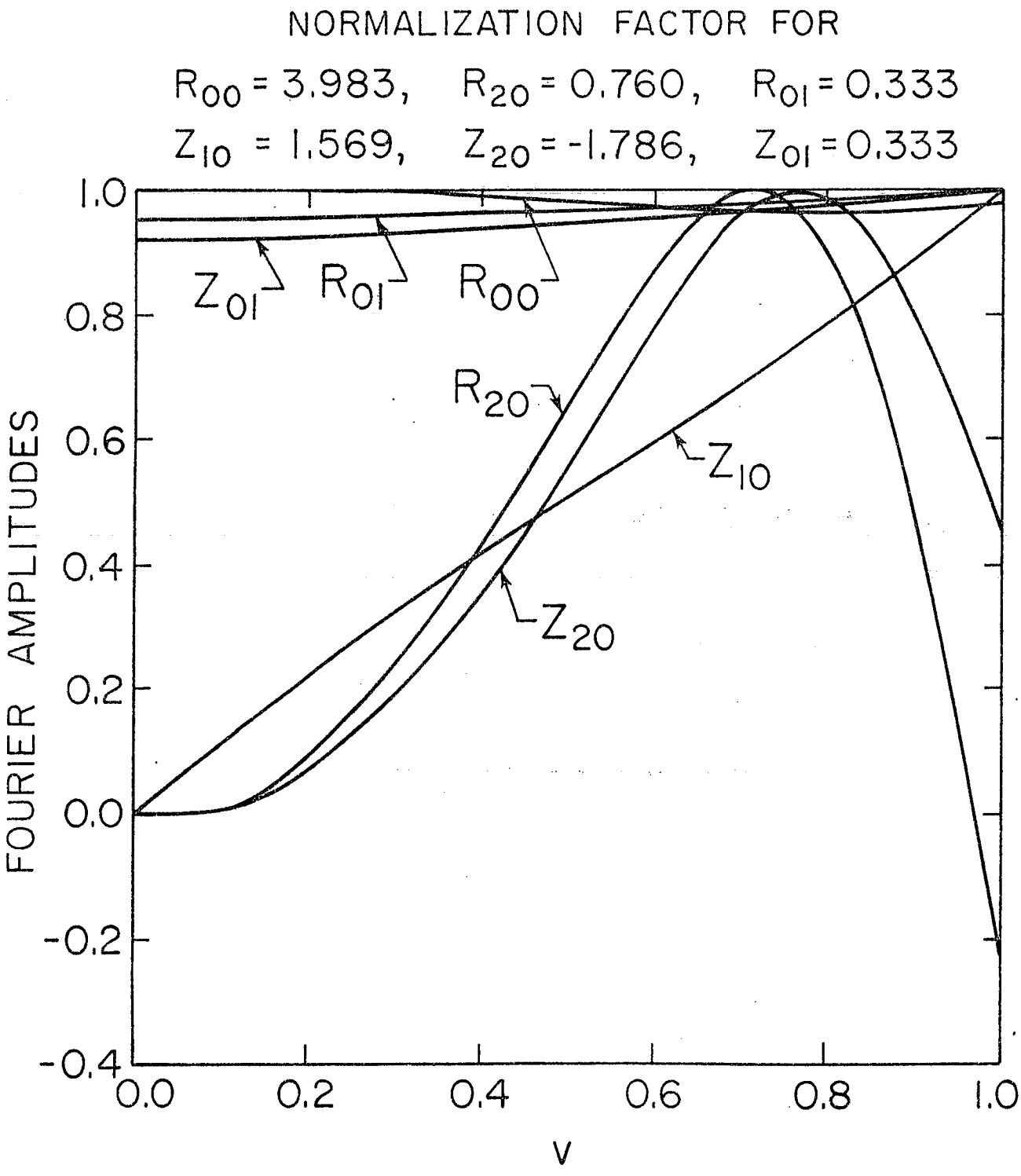
NORMALIZATION FACTOR FOR
$R_{00} = 3.983$, $R_{20} = 0.760$, $R_{01} = 0.333$
$Z_{10} = 1.569$, $Z_{20} = -1.786$, $Z_{01} = 0.333$
FOURIER AMPLITUDES
V
Z_{01}
R_{01}
R_{00}
R_{20}
Z_{10}
Z_{20}
1.0
0.8
0.6
0.4
0.2
0.0
-0.2
-0.4
0.0
0.2
0.4
0.6
0.8
1.0

FIG. 10